THE PRESSURE-INDUCED FUNDAMENTAL VIBRATIONAL SPECTRUM OF CHLORINE AT 298°K

MAYNARD J. CLOUTER

15629

THE PRESSURE-INDUCED FUNDAMENTAL VIBRATIONAL SPECTRUM OF CHLORINE AT 298°K.

by

© Maynard J. Clouter BSc.

Submitted in partial fulfilment
of the requirements for the degree of
Master of Science.

Memorial University of Newfoundland

September, 1962.

TABLE OF CONTENTS

CHAPTER I

INTRODUCTION

It has been shown, by investigations largely carried out at the University of Toronto,[1,2,3] that the symmetric diatomic molecules, oxygen, nitrogen and hydrogen, which normally do not exhibit absorption at their vibrational and rotational frequencies, can be rendered active in absorption at high densities and in high density mixtures with foreign gases. This phenomenon is referred to as "pressure induced absorption", and is attributed to the induction, during molecular collisions, of dipole moments in the electronic configurations of the molecules.

In the case of hydrogen, the investigations of the fundamental vibrational band have been particularly extensive. Experiments with the pure gas have been carried out up to pressures of 5000 atmospheres at 300°K [3] and to lesser pressures at temperatures varying from 40°K to 423°K. The absorption has also been studied in H_2- He, H_2- A and H_2- N_2 mixtures at various temperatures.

These studies have shown that the integrated absorption intensity, $\int A' d\nu$, in the induced fundamental band of hydrogen, satisfies the relation:

$$\int A' d\nu = \alpha = \alpha_1 \rho_0 \rho_p + \alpha_2 \rho_0 \rho_p^2 + \cdots$$

The absorption coefficient, $A'(\nu)$, is defined for given ν, by Beer's Law:

$$I = I_0 \exp(-A'\ell)$$

ℓ being the optical path length. The quantities, ρ_a and ρ_p are the absorbing and perturbing gas densities, respectively; it is assumed that $\rho_a << \rho_p$. For the pure gas, $\rho_a \equiv \rho_p$. The two constants α_1 and α_2 are called the "binary" and ternary" absorption coefficients, respectively.

It has been determined that the structure of the induced fundamental band of hydrogen is the same as that expected on the basis of the quantum mechanical selection rules for the Raman Effect. The band consists of a vibrational component, or Q-branch, corresponding to the transition v=0→v=1 with $\Delta J=0$ (v and J being the vibrational and rotational quantum numbers, respectively), and two rotational components, the S-branch and the O-branch corresponding, respectively, to the transitions v=0→v=1, $\Delta J=+2$ and v=0→v=1, $\Delta J=-2$.

A theory describing the induced absorption in homonuclear diatomic molecules has been developed by Van Kranendonk[14,15,16]. This theory has been very successful in describing the quantitative aspects of the absorption in hydrogen.

The molecules studied so far, however, have been of relatively low mass and it was consequently considered of interest to extend these investigations to heavier molecules, or to a series of molecules which covers a wide range of masses. The halogen series (fluorine, chlorine, bromine and iodine) is a particularly interesting case since all members

of the series are homonuclear diatomic molecules with similar chemical properties. Their molecular masses extend from 38 for F_2 to 254 for I_2.

Fluorine is a very chemically reactive substance so that the difficulty and danger of containing and handling it at high pressures precluded its use. Bromine and iodine are, respectively, liquid and solid at room temperature and would have to be handled at elevated temperatures to achieve a high pressure gas. In addition, the fundamental bands of bromine and iodine would be expected to occur in the spectral region beyond 30 microns which is not a convenient region for a preliminary investigation.

Chlorine is gaseous at room temperature up to an absolute pressure of about 100 p-s-i and although it is a chemically reactive substance it was chosen as being the most suitable for the present research.

This investigation was designed to observe the pressure induced fundamental rotation-vibration band of chlorine in the pure gas with the object of determining to what extent the previously mentioned theory could account for the observations.

CHAPTER II

APPARATUS AND EXPERIMENTAL METHOD

A. Absorption cell.

The experiments with pure chlorine gas were carried out using the one meter transmission cell shown in Figure (1). The first gas mixture experiments were carried out with a similar high pressure cell with about a 10 cm optical path, but it was found that the pressures necessary for the attainment of significant absorption were well above the maximum that the potassium chloride crystal windows could withstand. The final gas mixture experiments were consequently done with the same one meter cell as was used in the pure gas experiments.

The body, A, of this cell was a one meter length of iron pipe of 0.5 cm wall thickness with an outside diameter of 2.0 cm, containing a tight fitting tubular Pyrex glass light guide, B. Stainless steel fittings, C, were threaded on each end of this pipe and sealed against teflon washers, D. The stainless steel window plate, E, containing a central circular aperture of 1/4 inch diameter was sealed into position against the teflon washer, F, by the closure nut, G. The window plate was polished on its inner surface to a flatness of about 10 λ of sodium light and the window was cemented to this surface. The

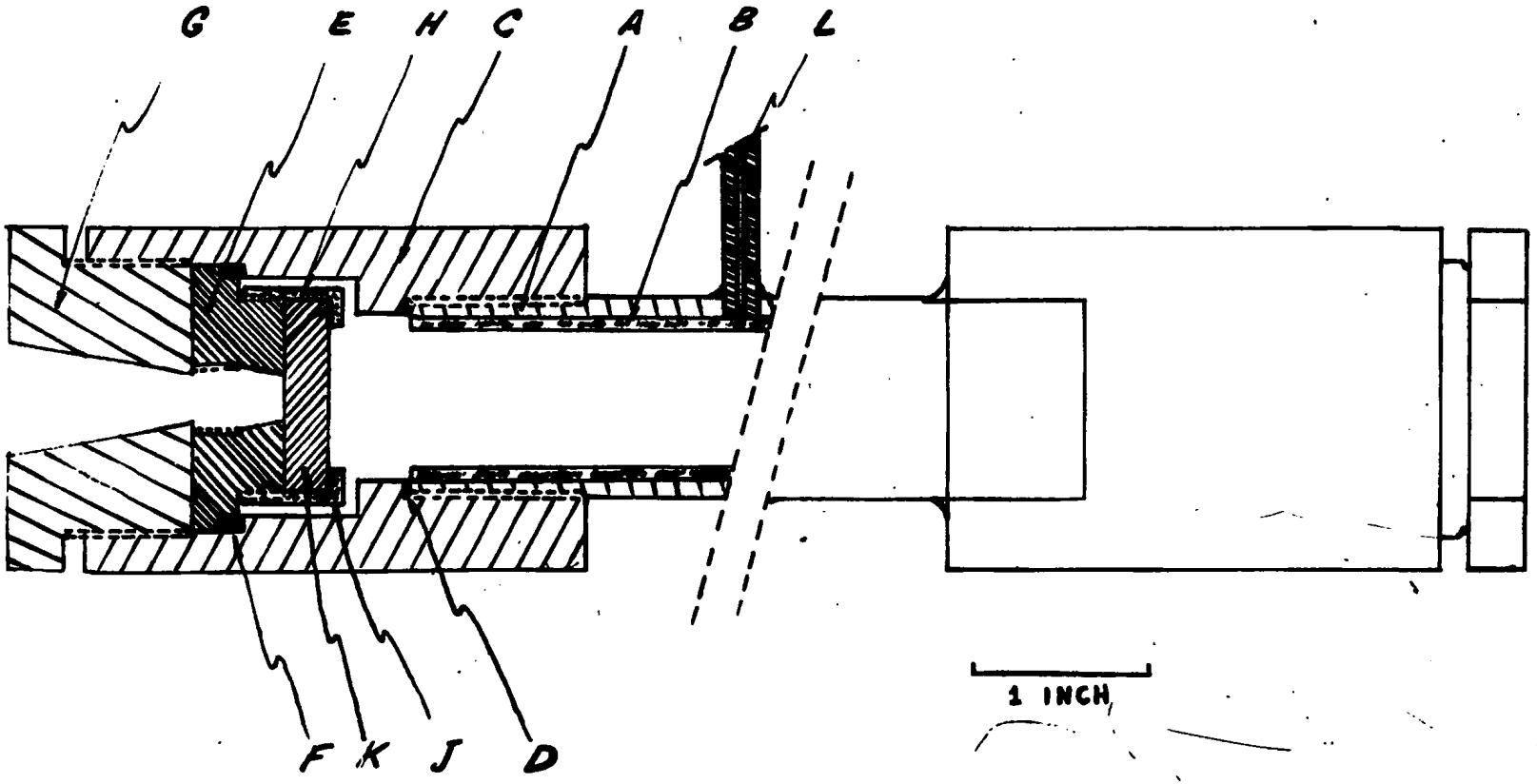

Figure (1): One meter transmission cell.

window plate was fitted with a cap, H, which, together with the teflon gasket, J, retained the window, K, in position and prevented damage to the window-to-window plate pressure seal during evacuation of the cell.

The inlet tube, L, was made of chrome-molybdenum steel with an outside diameter of 1/4 inch and a bore of 1/16 inch. It was first threaded into the cell body and then brazed to make a pressure tight connection.

Before assembling the cell, all parts were carefully cleaned in ethyl ether and rinsed with carbon tetrachloride.

B. Cell windows.

In preliminary investigations of the pure gas, both potassium bromide and caesium bromide were used as window materials because of their high transmission in the 18 micron spectral region. It was subsequently discovered, however, that chlorine reacted slowly with both materials, resulting in the formation of what was presumed to be potassium chloride and caesium chloride on the surfaces of the windows. This reaction did not prove to be troublesome in the low pressure, pure gas experiments but in the higher pressure, gas mixture experiments the formation of chloride deposits took place much more rapidly resulting in errors both in the chlorine density and the background intensity.

In this case, the bromide windows were replaced by potassium chloride windows to avoid the reaction problem, although the latter material did not transmit as well for wavelengths greater than 20 microns.

Several methods of polishing the various windows were tried but it was found that the combination of polish and flatness necessary for a good seal against the cell window plate was most easily achieved by means of the brass polishing tool shown in Figure (2). The overall diameter of this tool was 3 inches with a depth of about 1.5 inches. The central hole was machined to a diameter 1/64 inch greater than that of the windows which was 1 inch. A second off-centre hole, 3/4 inch in diameter, was then bored and a slot milled across the diameter of the central hole to the circumference of the second, thus providing a flexible hinge for clamping the window by means of the screw.

Most of the alkali halide crystal blanks used had irregularities in their surfaces which necessitated grinding. This was done with the crystal blank mounted in the polishing tool and projecting beyond its surface by about the thickness of a sheet of paper. The preliminary grinding was done using a fine grade of carborundum paper resting on a flat glass plate. Depending on the depth of the faults in the crystal blank surface, it was often necessary to repeat this grinding process two or three

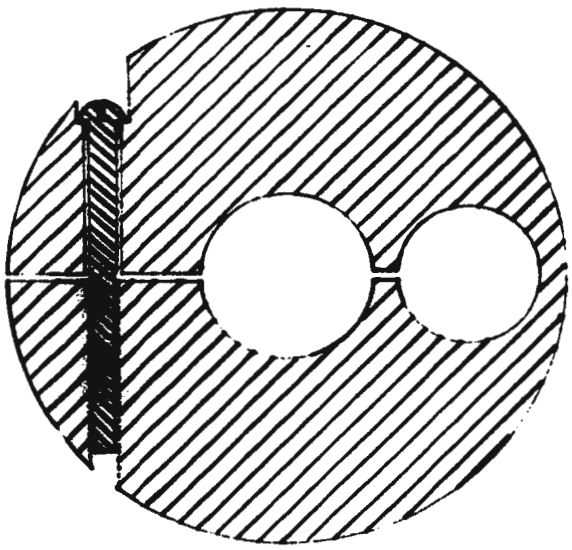

Figure (2): Window polishing tool

times. A second grinding process employing fine carborundum powder on a flat glass plate served to remove the scratches left by the first process.

The polishing surface used was a chamois skin. It was treated by first dusting it li ;htly with cerium oxide powder, and then soaking it in water and allowing it to dry until just slightly damp. Without disturbing the window in its mount after the grinding process, it was found that no more than 5 minutes polishing was necessary to produce a good polished surface without destroying its flatness. Since the windows were used in the infra-red, it was not considered necessary to obtain a high polish, but it was found that this could be achieved by prolonged polishing with the window recessed slightly into the tool to preserve the flatness.

Because of the chemical reaction problem, considerable difficulty was experienced in cementing the windows to the window plate. Both rubber cement and General Electric "Glyptal" cement were tried, but the "Glyptal", apparently because of its superior hardening properties, was found to be more resistive to reaction and gave a better seal. In cases where it was necessary to remove sealed windows without damaging them, it was found that soaking for 24 hours in ethyl ether would dissolve the "Glyptal". In the high pressure, gas mixture, experiments the reaction with the "Glyptal"

proved to be more penetrating but in most cases did not proceed far enough to cause leaks. In an effort to circumvent this problem, several attempts were made to isolate the cement from the gas by using both paraffin wax and "Silicone" stopcock grease but both these materials were decomposed by chlorine at high pressure.

The behaviour of potassium chloride windows under pressure was investigated using a 10 cm high pressure cell similar in construction to that of Figure (1), and the optical lever assembly of Figure (3).

In Figure (3), the wooden base, A, containing a central hole of about 1/8 inch diameter, was made to fit tightly into the aperture of the cell closure nut, B. The polystyrene lever arm, C, was supported by the fulcrum, D, and kept from oscillating by the rubber bands, E. The lever arm was activated by the glass rod, F, resting on the cell window and passing through the central hole of the base, A. A mirror, H, was cemented to the lever arm and a light beam was reflected from it on to a vertical scale at a distance of about 9 meters. It was found that this apparatus could detect a minimum window extrusion of 0.005 mm.

A representative window about 9 mm thick was sealed into one end of the cell, a brass disc being substituted for the second window, and pressure was

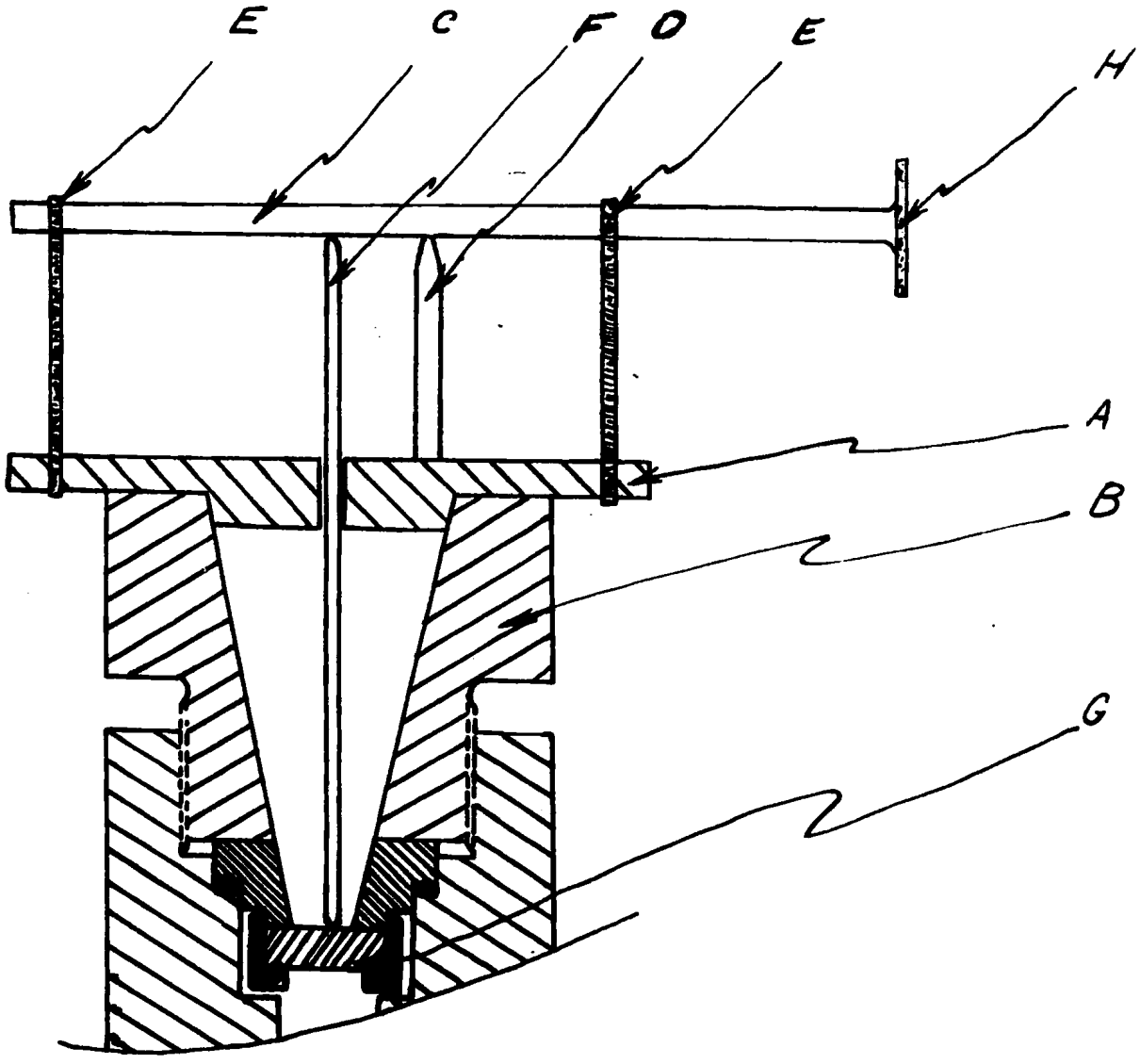

Figure (3): Optical lever assembly.

applied with oil from a hydraulic press. The extrusion was measured over 10 minute intervals for each pressure increase of 200 p-s-i.[4] The curve of Figure (4) shows the results obtained. The maximum extrusion was about 1 mm. It was found that pressures up to 10,000 p-s-i could be attained safely but between 8,000 p-s-i and 9,000 p-s-i the window fractured on the free surface so that 9,000 p-s-i was considered the maximum pressure for undistorted signal transmission.

C. Compression apparatus.

In the pure gas experiments, pressures up to a maximum of 90 p-s-i, corresponding to the vapor pressure of liquid chlorine at room temperature, were obtained by bleeding the gas from a thermal compressor containing about 50 cc of liquid chlorine.

The thermal compressor, shown in Figure (5), was made of stainless steel and had a maximum capacity of about 75 cc. The threaded plug, P, could be removed to facilitate cleaning. The inlet connection was a standard "Aminco" type using 3/8 inch outside diameter steel tubing.

In the gas mixture experiments, pressures of argon, nitrogen and helium in excess of cylinder pressure were attained by means of the gas compressor shown in Figure (6). This compressor is very similar in design to

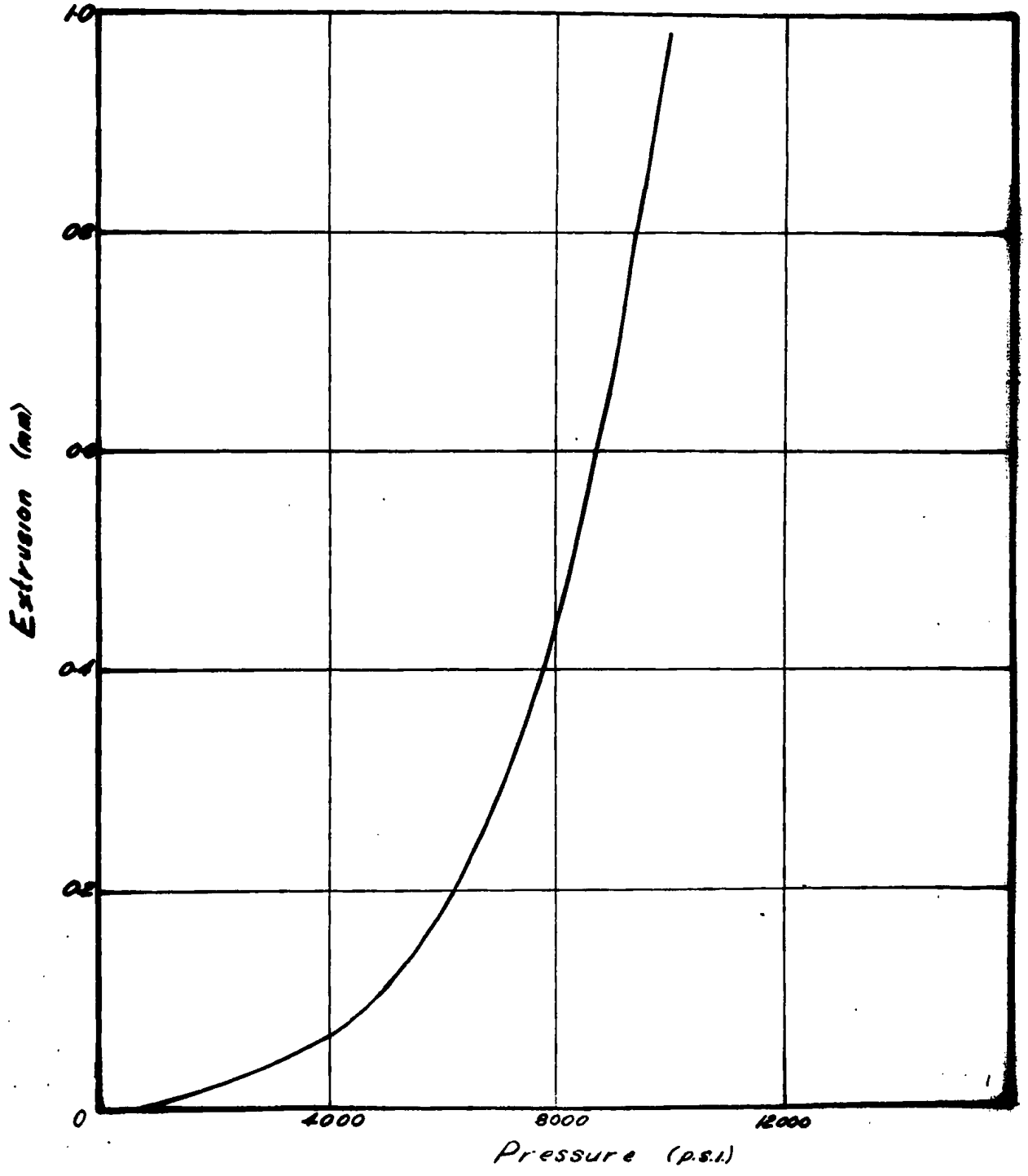

Figure (4): Extrusion of KCl windows under pressure.

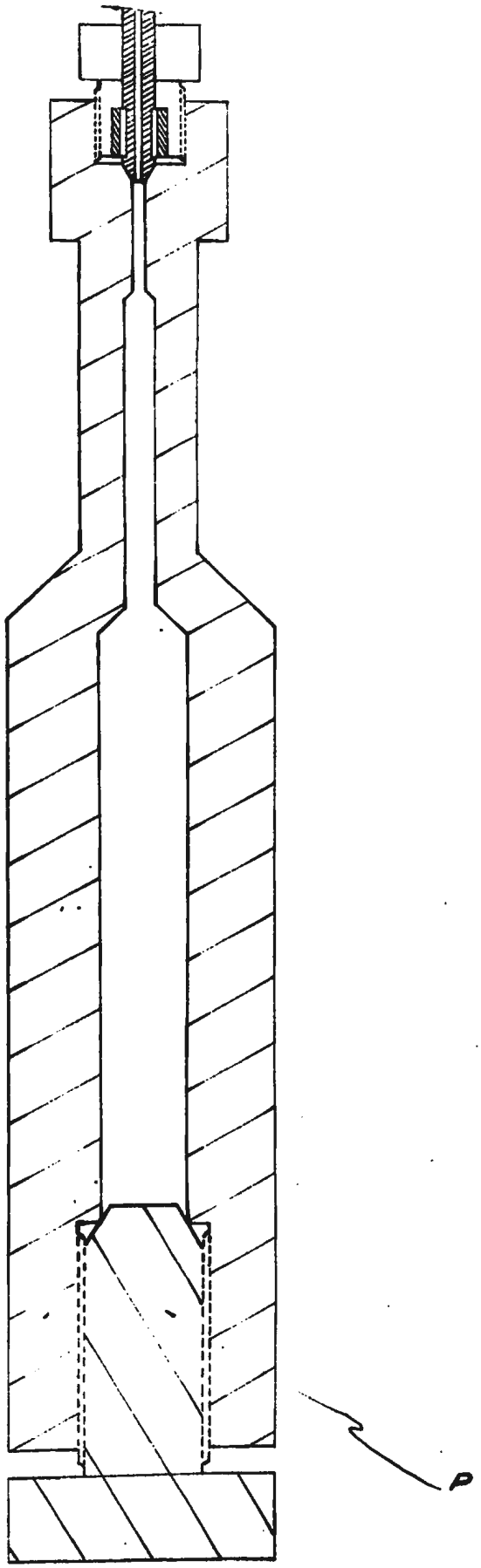

Figure (5): Thermal compressor.

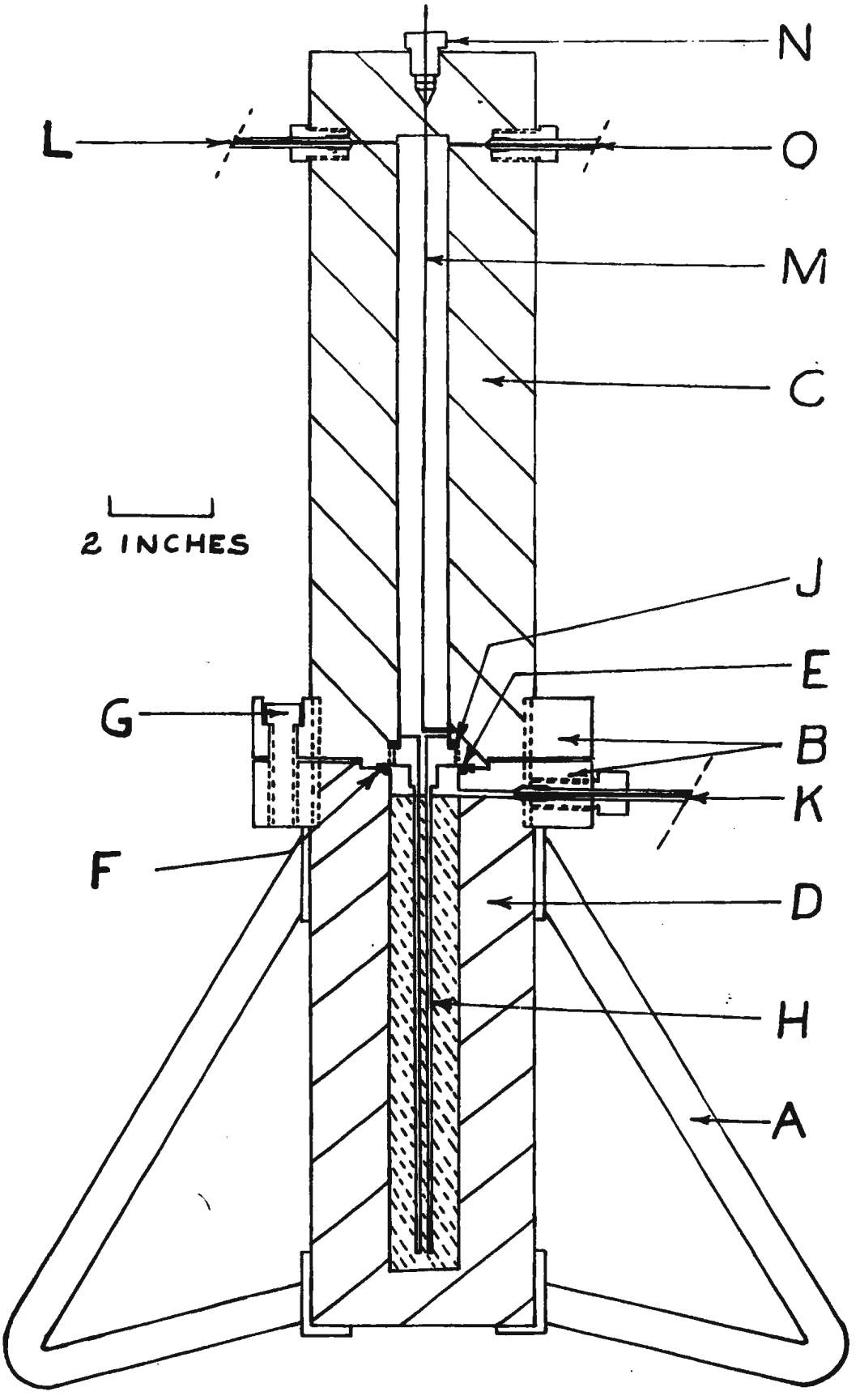

Figure (6): Mercury column gas compressor.

that of A. Carswell.[5] With the exception of the supporting stand, A, and flanges, B, the compressor was constructed wholly of stainless steel. The upper cylindrical chamber, C, was about 3.2 cm in inside diameter providing a maximum gas volume of about 342 cc. The lower chamber, D, initially filled with mercury, was about 3.8 cm in inside diameter with a net volume of 328 cc. The two sections were sealed together with a rubber O-ring, E, and stainless steel backing ring, F, together with six drop forged bolts, G, through the flanges, B. The dip-tube, H, was threaded into the lower end of the top section and sealed against the teflon gasket, J. The oil inlet, K, was of a standard "Aminco" type using 3/8 inch outside diameter steel tubing. It was threaded directly into the lower flange and seated against the cylinder, D.

With the valve on the oil line closed, the upper chamber was both evacuated and filled with gas through a needle valve at L. Compression of this gas was then achieved by forcing oil into the lower chamber thus raising the mercury to any desired level in the upper chamber. A platinum wire, M, of uniform linear resistance, grounded to the compressor body at the lower end of the top section and led to the outside through an insulated compression fitting, N, was used to monitor the height of the mercury column during the compression operation so as to avoid overflow of mercury into the accompanying

apparatus in cases where the outlet valve at O was kept in the open position.

In the mixture experiments, the gas pressures of argon, helium and nitrogen were measured with a stainless steel Bourdon gauge, and, in the case of pure chlorine, a similar gauge was used which was filled with oil and isolated from the rest of the system by a flexible diaphragm made of "Hastelloy-C" alloy. The Bourdon gauges were calibrated by comparing them with laboratory test gauges which were accurate to 0.25% of full scale deflection.

D. Purification of gases.

Spectroscopic analysis of the commercial chlorine used in these experiments revealed the presence of several impurity bands, the two most important of which were due to chloroform and carbon dioxide at 13.66 microns and 14.97 microns, respectively. The chloroform band was later found not to interfere with the observations, but it was considered necessary to remove the carbon dioxide.

Because of the high chemical reactivity of chlorine, it was apparent that this could not be done by chemical means. Furthermore, it could not be done by a simple arrangements of low temperature traps because carbon dioxide does not condense above -78°C whereas chlorine is liquid at -35°C. It was consequently necessary to

design the low temperature distillation apparatus shown in Figure (7).

Except for the connection to the cylinder supply, which was heavy walled "tygon" tubing, this apparatus was constructed wholly of glass. The mercury of the manometer was protected to some extent from the effects of chlorine by a small amount of pure H_2SO_4 on top of the mercury column.

Reservoir A of this apparatus was maintained at -78°C with a bath of dry ice and acetone, and reservoir B at -188°C by means of liquid air. After evacuating the system, all stopcocks were closed except #1 and #2. The gas was then admitted through a needle valve from the cylinder supply until a pressure of 20 to 30 cm was registered on the manometer. Stopcock #4 was then opened, thus giving access to the liquid air trap, until the pressure dropped to about half its initial value. Thus operated, traps A and B filled with chlorine at approximately the same rates. However, because of the greater mobility of the carbon dioxide molecule compared to the chlorine molecule, and also, since the carbon dioxide could condense in trap B but not in trap A, trap B collected a greater portion of the carbon dioxide impurity than did trap A.

With reservoir A filled, the supply was shut

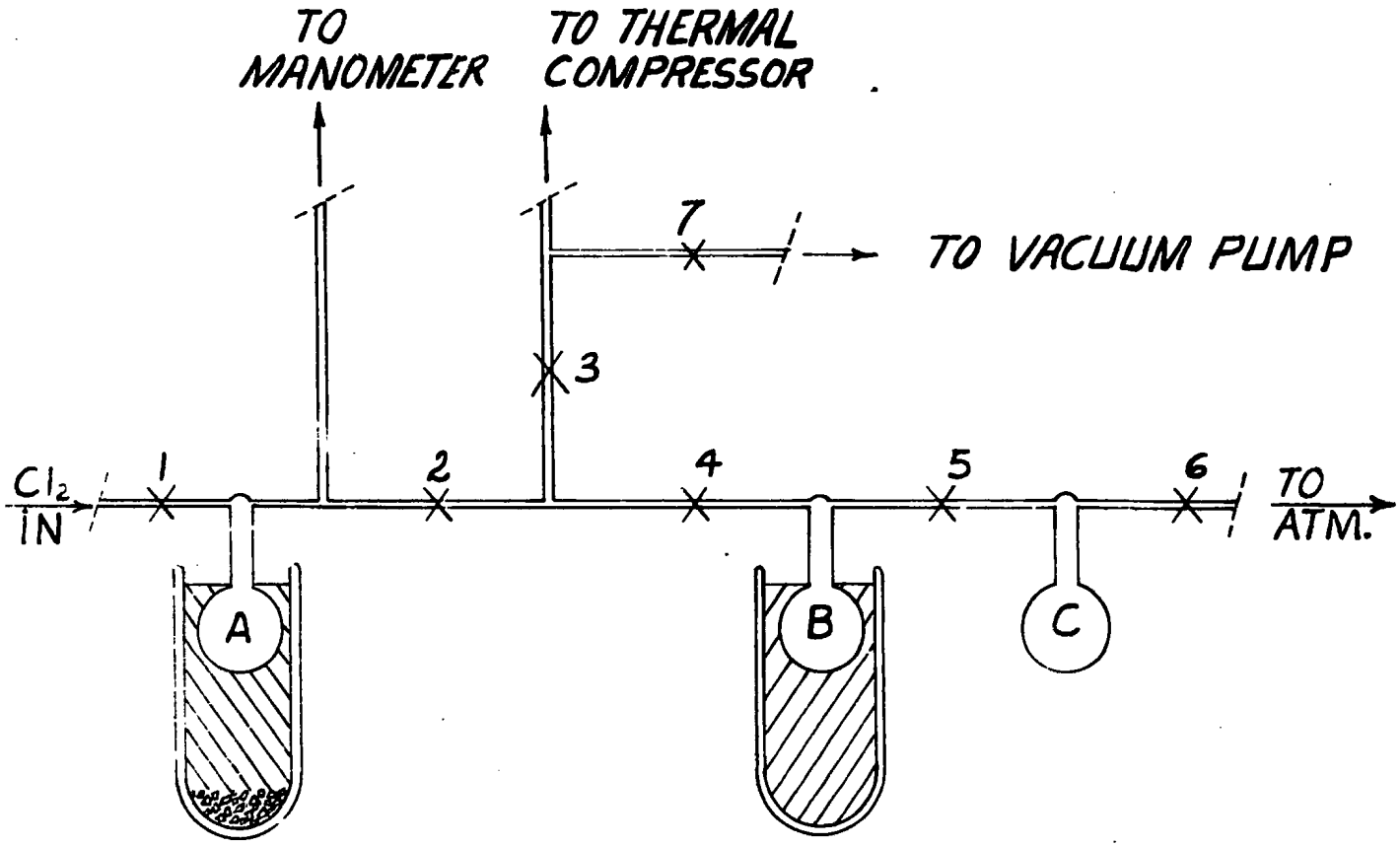

Figure (7): Purification system for chlorine.

off and the contents of trap B discarded by warming and condensing into trap C from which it was eventually expelled to the outside air. With stopcocks #1 and #5 closed, the contents of trap A were then solidified and the system opened to the vacuum pump for a period of two to three hours. Trap B was then cooled to liquid air temperature again and the contents of trap A allowed to rise to dry ice temperature. With stopcocks #1 and #4 open and the vacuum pump shut off at stopcock #3, it was assumed that any carbon dioxide still dissolved in the liquid chlorine would diffuse more rapidly into trap B than would the chlorine itself. The initial volume in trap A was about 120 cc. The process was allowed to continue for several hours, trap B being emptied periodically, until about 60 cc remained in trap A. All but 10 cc of this amount was then transferred to the thermal compressor for storage.

From approximate measurements made on the 14.97 micron carbon dioxide band, this purification method was found to reduce the CO_2 content from 4.5% per volume to 0.25% per volume.

Purification of the helium, nitrogen and argon used in the gas mixture experiments was done by passing the gases through a series of traps before entering the compressor. In the case of helium a liquid air trap was

considered sufficient. The nitrogen was liquified in a liquid air trap and then slowly forced from the trap into the compressor under cylinder pressure. The argon was passed over silica gel and soda lime, to remove water and carbon dioxide, respectively, and then through a dry ice trap.

E. Pressure-density data.

Pressure-density relations for pure chlorine were derived from the following equation given by K. Wohl[6] which was stated to be correct to 1% for all stable gaseous states.

$$\pi = \frac{3.75\theta}{\phi - 1/4} - \frac{6}{\phi\theta(\phi - 1/4)} - \frac{4}{\theta^{4/3}\phi^3}$$

π, θ and ϕ are defined in terms of the critical constants as:

$$\pi = \frac{P}{P_c}, \quad \theta = \frac{T}{T_c}, \quad \phi = \frac{V}{V_c} = \frac{\rho_c}{\rho}$$

The values $T_c = 416°K$ and $P_c = 78$ atmospheres were given for the critical temperature and critical pressure but no value for the critical density was stated. The value of this constant was taken from the Chemical Rubber Publishing Company "Handbook of Physics and Chemistry" where it was listed as $\rho_c = 0.573$ gm/cm^3.

For purposes of comparison, the pressure-density curve for chlorine was also derived from the Van der Waals equation of state;

$$(P + a/V^2)(V - b) = RT$$

using the values of the constants; a=6.40 litre^2-atm/mole^2 and b=0.0551 litre/mole.[7]

The difference between the two curves up to a density of 7 Amagat units was found to be less than 0.2% at 25° C. The density of a gas expressed in Amagat units is defined as the density of the gas divided by the density at NTP.

The pressure-density relations for nitrogen, argon and helium, were obtained from the literature.[8,9,10]

F. Spectroscopic apparatus.

All experiments in this research were performed with a recording Perkin-Elmer 12C spectrometer using a potassium bromide prism and thermocouple detector. The infra-red source was of the standard "Globar" type operated at about 200 watts from a Sorenson voltage regulator and barretted for extra current stability by three 200 watt tungsten filament lamps.

The standard optical arrangement used for the one meter absorption cell is shown in Figure (8). Radiation from the globar, A, was focused on to the window at one end of the cell, B, by the spherical mirror, C, which had

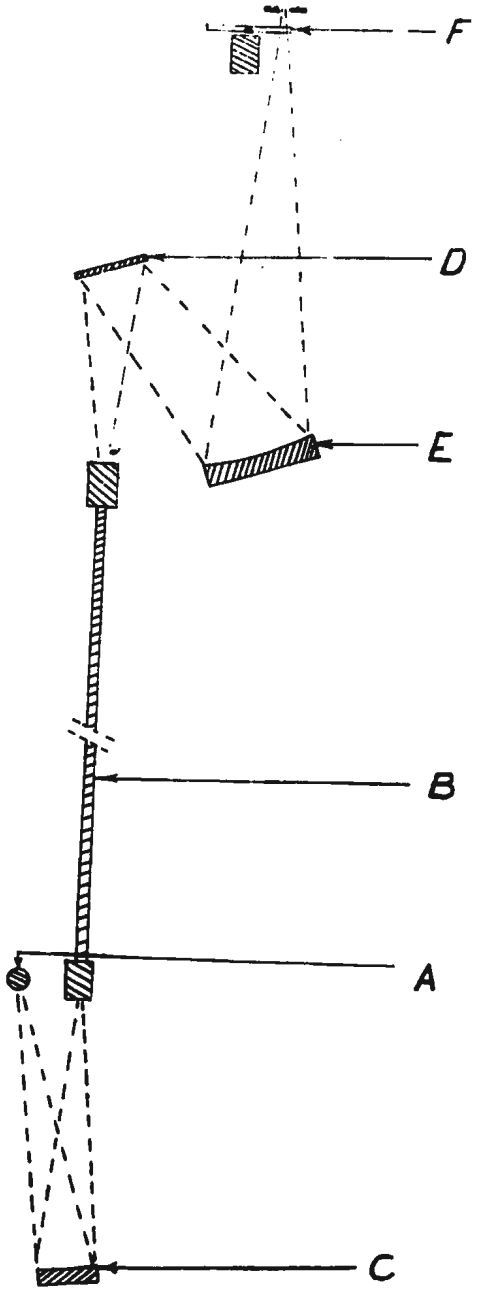

Figure (8): Optical arrangement for the one meter cell.

a radius of curvature of 18 inches. After traversing the cell, the radiation was reflected from the plane mirror, D, onto the spherical mirror, E, which brought it to focus on the spectrometer slits at a distance of 24 inches. The beam chopper at F was made of plexiglas to minimize detection of stray radiation in the visible and near infrared regions of the spectrum.

The spectrometer slit width was maintained at 0.5mm for the extent of the band. This resulted in a spectral resolution which varied from 9 cm^{-1} to 4 cm^{-1} over the band, being 5 cm^{-1} at the peak of absorption.

A frequency calibration for the spectral region from 15 to 22 microns was obtained by fitting a Hartmann dispersion formula[11] to the observed positions of the absorption bands of carbon dioxide (14.97μ) and atmospheric water vapor (19.01μ, 21.16μ). Observation of some emission lines of an oxy-acetylene flame[12] showed that the resulting calibration was correct to one half wave number in the region of interest.

At the beginning of each experiment it was necessary, because of the reaction problem, to purge the cell by filling it with chlorine at about 80 p-s-i and leaving it for a period of 12 to 24 hours till all reactions with residual organic impurities in the system became negligible. The remaining gas was then discarded and the cell opened to the vacuum pump for several hours.

With the cell evacuated, a recorder trace of the background radiation was taken and, subsequently, similar traces corresponding to different pressures of chlorine in the cell. At the end of the experiment, the cell was re-evacuated and a final background obtained. The position of infinite absorption on the recorder trace was also determined by filling the cell with 900 p-s-i of carbon dioxide.

In the gas mixture experiments, the cell was similarly purged, then filled with a base density of chlorine varying from 2 to 4 Amagat units. A recorder trace of the spectrum was then taken and used as the background for measuring the enhancement of the absorption after admission of foreign gases into the cell.

The foreign gases were admitted in short bursts through a needle valve close to the cell body so as to minimize back-diffusion of chlorine from the cell. When the desired gas mixture pressure was attained, it was necessary to wait for a period of 1 to 2 hours for the gases to mix before continuing with the experiment.

In reducing the data, all absorption traces were copied on the background trace and, with the aid of the frequency calibration, the absorption coefficient, $A = \log_{10} I_0/I$, where I_0 is the background intensity and I the intensity of absorption at frequency ν, was calculated at one wave number intervals and plotted against ν.

CHAPTER III

RESULTS AND DISCUSSION

Examples of the fundamental rotation-vibration absorption band of chlorine obtained in this research are shown in Figures (9), (10) and (11). The quantity ρ_a is the absorbing gas density in Amagat units, and ρ_p is the density of the perturbing gas. In the case of the pure gas, $\rho_a \equiv \rho_p$. The position of the $Q_1(0)$ line, as calculated from the molecular constants for Cl_2^{35} given in the literature (App. IA), is marked on the frequency axis.

In Figure (9), the contours, corresponding to a temperature of 298°K, for pure chlorine are shown for gas densities, ρ_a, varying from 1.49 to 6.80 Amagat units. Two maxima were resolved which, for ρ_a = 6.80 Amagat units, occur at 549 cm^{-1} and 576 cm^{-1}. The latter peak was found to move to higher frequencies with decreasing density whereas the former remained fixed. Also, the ratio of the peak intensities of these two maxima was found to vary from 1.7 : 1 to 1.0 : 1 for densities of 6.80 and 1.49 Amagat units, respectively.

The gas mixture bands of Figures (10) and (11), corresponding to a temperature of 298°K, are given for gas density ratios, $\rho_a : \rho_p$, varying from 0.009 : 1 to 0.02 : 1. These curves do not exhibit any definite structural features, except for the case of the low density Cl_2- A

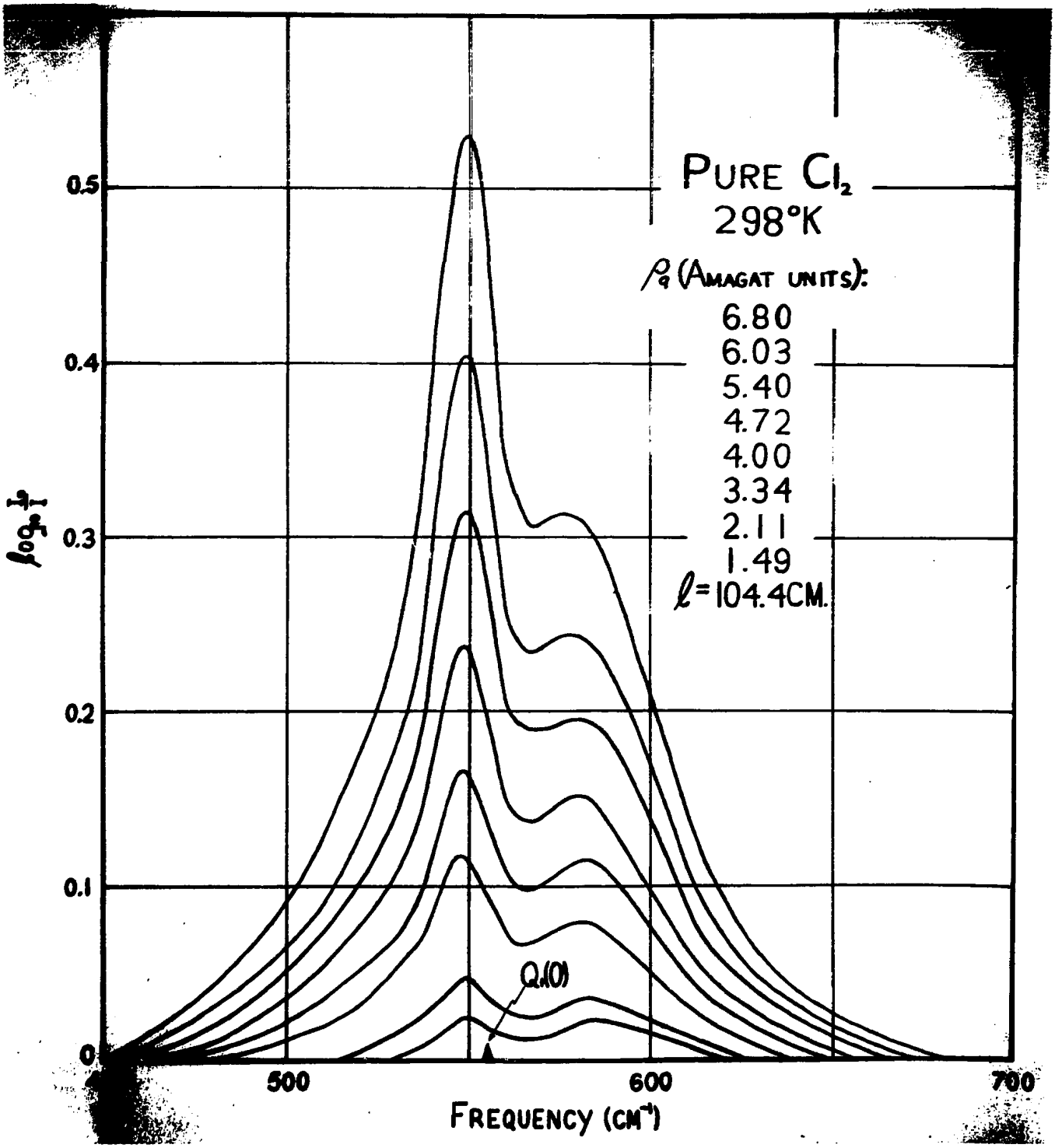

Figure (9): Absorption profiles of the fundamental band of pure chlorine at 298°K.

curves where two maxima were resolved. These latter curves, however, were not considered reliable because of the relatively low level of absorption. For higher densities, the contours for both the Cl_2-A and Cl_2-N_2 mixtures show only one rather broad peak at about 555 cm^{-1}.

An interesting feature of the experimental contours of Figure (9) is that the peak of the Q-branch does not occur at its calculated position. As given in Appendix ID for Cl_2^{35}, the maximum intensity line of the Q-branch, namely $Q_1(23)$, should occur at 555.39 cm^{-1}. The experimental peak for chlorine therefore shows a red shift of over 6 cm^{-1} from this position.

It is appropriate, at this point, to mention that the position of the experimental peak was fairly accurately determined since two series of experiments were carried out with the gas. In the first series, using unpurified chlorine, the high frequency side of the band above 600 cm^{-1} was obscured by absorption due to impurity carbon dioxide. The remainder of the band, however, including the peak of the Q-branch was well defined so that a comparison could be made when the second series of experiments was later done with the purified gas. It was then found that the peak of the Q-branch for all contours occured, within an experimental error of 1 cm^{-1}, at 549 cm^{-1}.

Since, however, the position (555.39 cm^{-1}) of

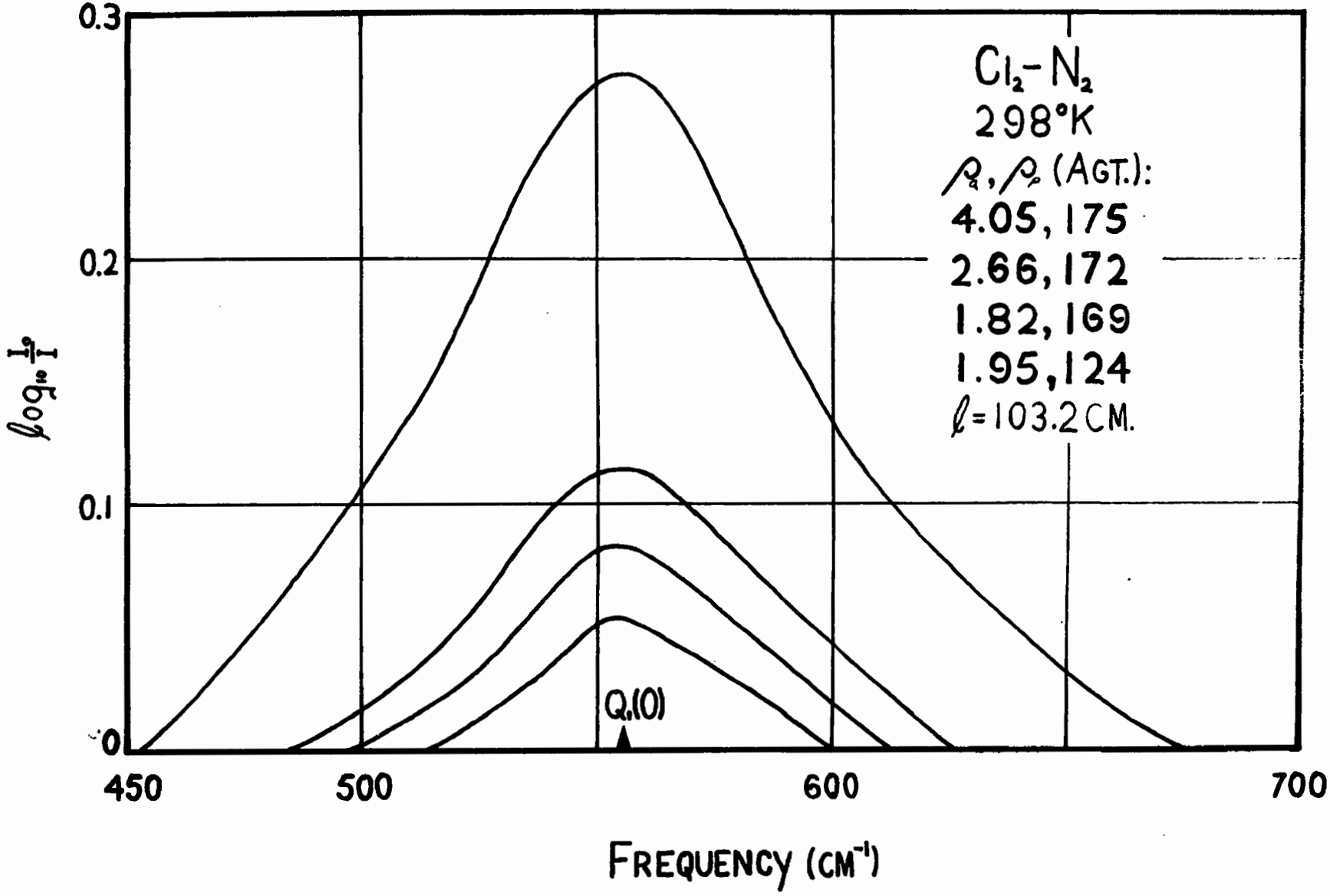

Figure (10): Absorption profiles of the fundamental band of chlorine for Cl_2-N_2 mixtures at 298°K.

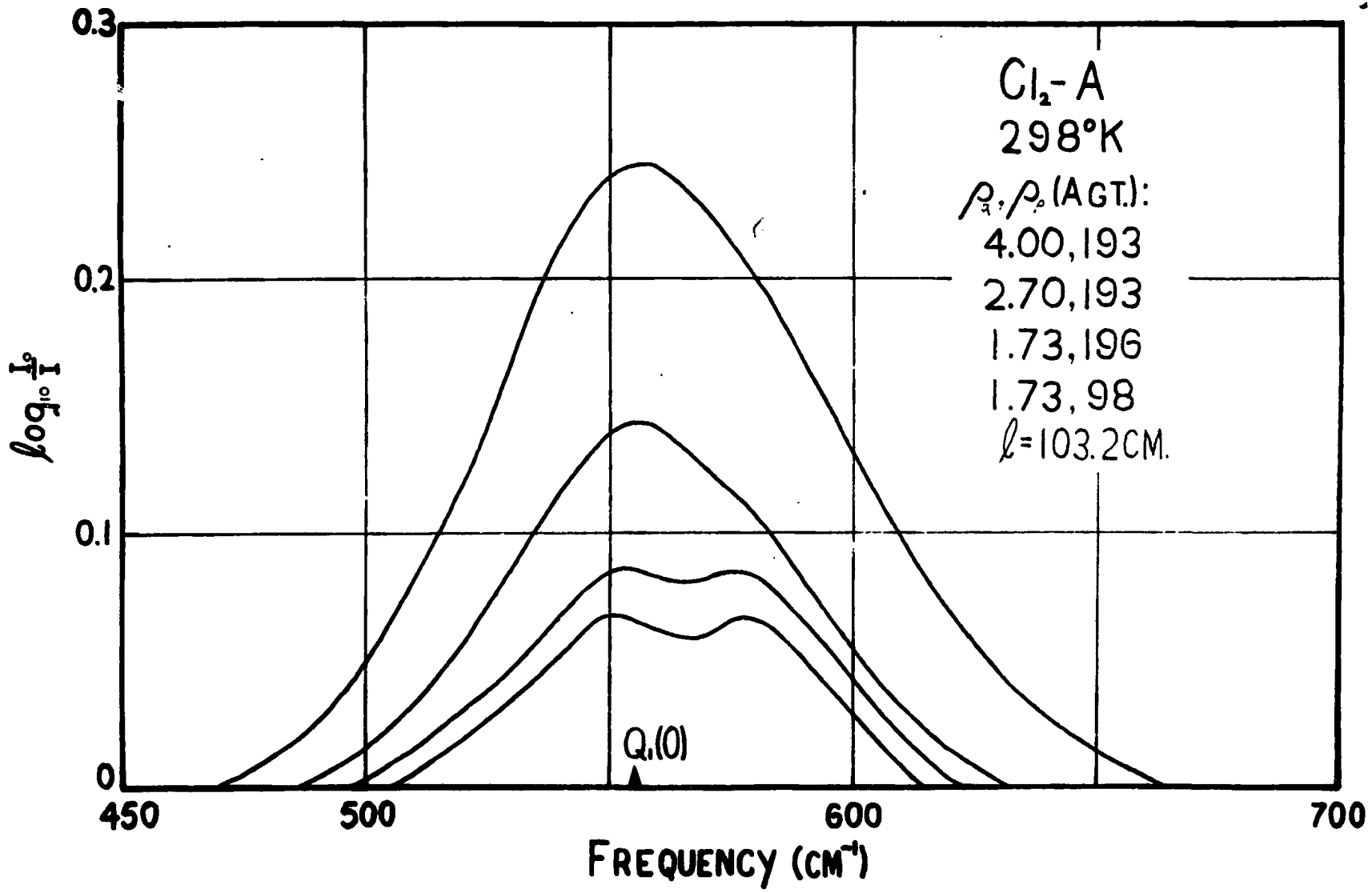

Figure (11): Absorption profiles of the fundamental band of chlorine for Cl_2-A mixtures at 298°K.

the peak was calculated on the basis of constants for Cl_2^{35}, and also, since the chlorine used was a normal mixture of the three isotopic molecules Cl_2^{35}, $Cl^{35}Cl^{37}$ and Cl_2^{37}, it was considered possible that the shift of the observed peak could be caused by the isotope shift to lower frequencies of the underlying absorption bands due to $Cl^{35}Cl^{37}$ and Cl_2^{37}. An attempt was consequently made to determine whether this was in fact the case by means of a method which will now be discussed.

The percentage abundances of the two stable isotopes of chlorine, namely Cl^{35} and Cl^{37}, are given in the literature[13] as 75.4% and 24.6%, respectively. Simple calculations show, assuming random association of these two isotopes into molecules, that normal chlorine should be composed of ~~75.1~~ 69.8% Cl_2^{35}, ~~20.3~~ 22.8% $Cl^{35}Cl^{37}$ and ~~5.6~~ 7.4% Cl_2^{37}.

The theory of pressure induced absorption of Van Kranendonk[14,15,16] describes the absorption intensity in terms of transient dipole moments induced, during molecular collisions, in the electronic configurations of the molecules. Small variations in nuclear mass can have only a slight effect on these charge distributions, so it may be assumed that, of the total absorption represented by each of the experimental contours of Figure (9), ~~75.1~~ 69.8% of each is due to the presence of Cl_2^{35}, ~~20.3~~ 22.8% is due to the presence of $Cl^{35}Cl^{37}$ and ~~5.6~~ 7.4% is due to Cl_2^{37}.

The absorption bands of $Cl^{35}Cl^{37}$ and Cl_2^{37} can be expected to be of slightly different shape from the band for Cl_2^{35} because of the effect of isotopic mass upon the rotational energy levels. In particular, the difference in shape will be most pronounced for the case of the $Cl^{35}Cl^{37}$ molecule which being non-symmetric will not exhibit the alternation of intensities for successive rotational lines which is characteristic of the bands for both Cl_2^{35} and Cl_2^{37}.

However, the most important difference of the $Cl^{35}Cl^{37}$ and Cl_2^{37} bands, as compared with the Cl_2^{35} band, is due to the vibrational isotope shift. As calculated in Appendix IE, this will shift the peaks of these bands by about 8 cm^{-1} and 15 cm^{-1}, respectively, to the low frequency side of the calculated position for Cl_2^{35}.

In the present considerations, only the vibrational isotope shift is taken into account. No attempt was made to compensate for the rotational isotope effects since they are probably of lesser magnitude than the vibrational isotope effect, and the experimental contours were not considered accurate enough to justify such corrections.

Since no experimental information (other than the results of this research) were available, it could only be assumed, to a first approximation, that the shapes of the

$Cl^{35}Cl^{37}$ and Cl_2^{37} bands were the same as the experimental contours of Figure (9). The most accurate of the experimental contours, that is, the curve corresponding to a density of 6.80 Amagat units was therefore used as a model. From it two other curves were constructed by multiplying the ordinates by ~~0.203~~ 0.228 and ~~0.066~~ 0.074, respectively, at 1 cm^{-1} intervals. These curves consequently represented ~~20.3%~~ 22.8% and ~~6.6%~~ 7.4%, respectively, of the total absorption and were taken to approximate the shapes of the absorption bands due to $Cl^{35}Cl^{37}$ and Cl_2^{37}. These latter curves were then positioned with appropriate peak frequencies as calculated from the "Isotope Effect" in Appendix IE, and the sum of their ordinates, for given ν , was subtracted from the experimental curve. The resulting curve was presumed to correspond to the absorption due to Cl_2^{35}.

If the experimentally observed shift of 6 cm^{-1} was in fact due to the isotope shift of the $Cl^{35}Cl^{37}$ and Cl_2^{37} bands, then the procedure as outlined above should produce a resultant curve with its peak frequency at the calculated position, 555.39 cm^{-1}, for Cl_2^{35}. However, this was not the case. Rather, the peak of the resultant was still shifted by about 5 cm^{-1} to the red side of its calculated position. In fact, the peak position of the resultant curve was found to be quite insensitive to the peak positions of the synthetic $Cl^{35}Cl^{37}$ and Cl_2^{37} curves. Shifting the latter curves by as much as 6 cm^{-1} to either

side of their calculated positions tended to shift the peak of the resultant into coincidence with that of the experimental curve.

It was therefore assumed that this 5 cm^{-1} red shift should apply to the contours of all species, Cl_2^{35}, $Cl^{35}Cl^{37}$ and Cl_2^{37}, in addition to the isotope shifts.

With this point in mind and with the object of obtaining greater accuracy in the shape of the resultant Cl_2^{35} curve, the previously outlined procedure was repeated in a slightly different manner. Instead of constructing the $Cl^{35}Cl^{37}$ and Cl_2^{37} curves from the experimental contour, they were constructed by using the previously obtained resultant Cl_2^{35} curve as a model, since it could be expected to be a better approximation of the true shape. The synthetic $Cl^{35}Cl^{37}$ and Cl_2^{37} curves were then positioned with their peak frequencies at 5 cm^{-1} to the red side of their calculated positions and then subtracted from the experimental curve. The result was a Cl_2^{35} curve different in shape from the previous one and with its peak shifted by about 5 cm^{-1} to the red side of its calculated position.

Finally, the procedure was repeated once more, using the Cl_2^{35} curve resulting from the second operation as a model for constructing the $Cl^{35}Cl^{37}$ and Cl_2^{37} curves, and positioning them 5 cm^{-1} lower in frequency than their calculated values. The final set of curves is shown in Figure (12). It was found that the Cl_2^{35} curve shown in

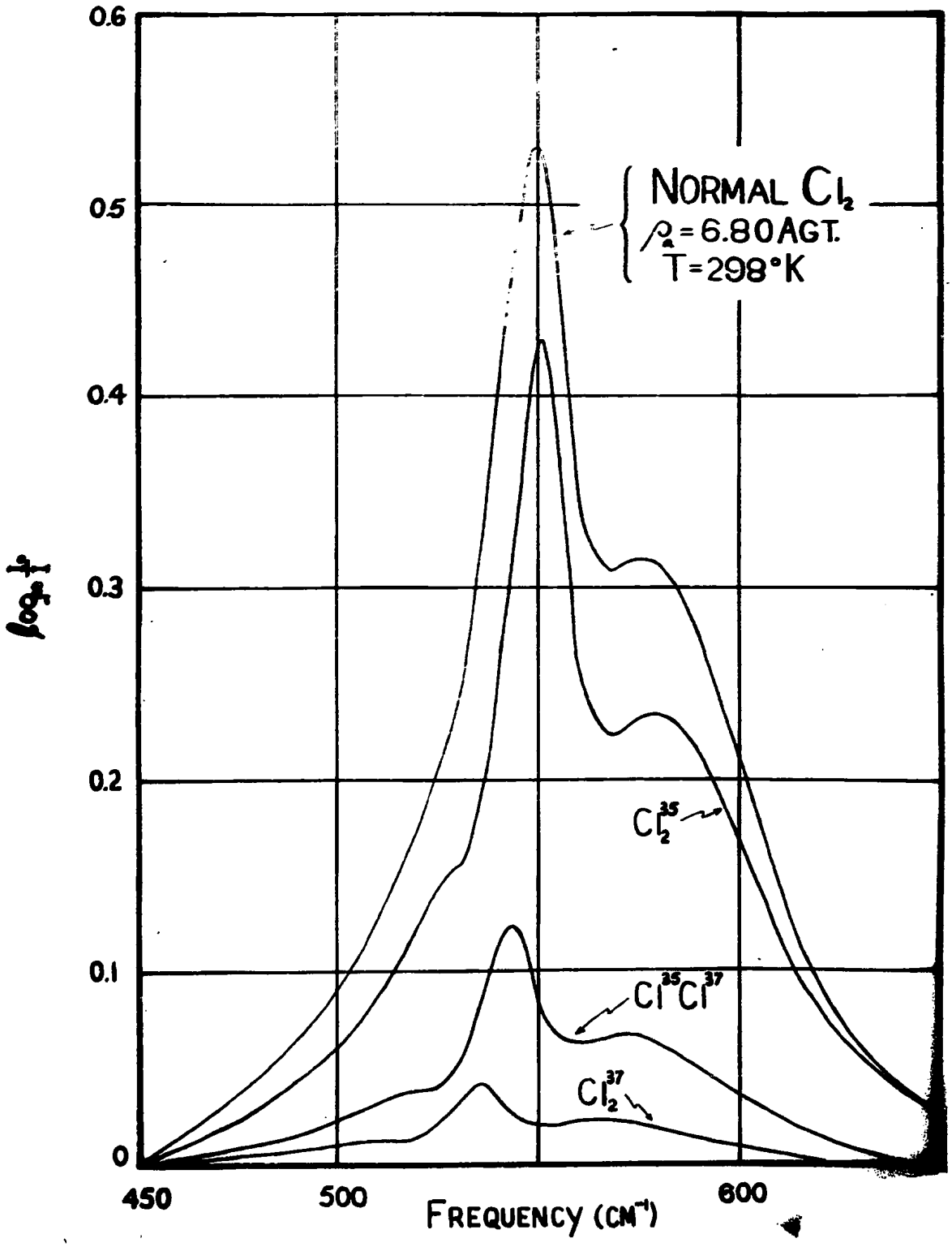

Figure (12); Isotopic analysis of pure chlorine contour at 298°K.

this Figure was only slightly different from that obtained from the second operation so that it was considered the best obtainable approximation of the shape of the absorption contour for the isotopically pure gas.

The results of this analysis would seem to indicate that there is a definite red shift of the induced vibrational absorption of chlorine compared with that predicted for the free molecule. This shift may be attributable to a perturbation of the vibrational energy levels of the absorbing molecule during interaction with a perturbing molecule. Because the shift is red, it appears that the interaction is taking place predominantly in the attractive region of the intermolecular potential.[17,18,19] From simple considerations the shift should be temperature dependent, because of the change in the distance of closest approach of the interacting molecules with temperature. This is a postulate which should be tested by further experiments.

An analysis of the branch structure of the final Cl_2^{35} curve was made using a method based on work done by Kiss.[20] He determined that the shape of the individual pure rotational lines of hydrogen could be represented by the relations

$$I^- = I^+ \frac{\nu^-}{\nu^+} \exp\left(-\frac{hc}{kT} \Delta\nu\right) \qquad (3.1)$$

$$I^+ = I_0 \frac{\delta^2}{\delta^2 + (\Delta\nu)^2} \qquad (3.2)$$

The significance of the quantities in these equations is shown in Figure (13).

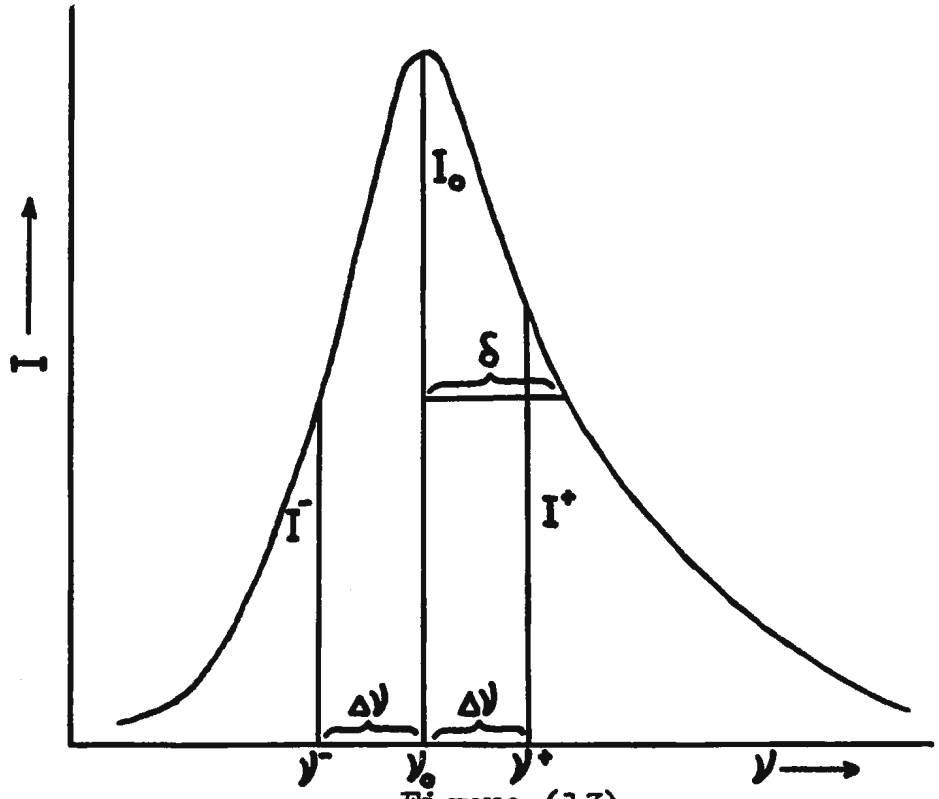

Figure (13)

T is the absolute temperature and δ is the half width of the higher frequency half of the line. It was further shown by Hunt [21] that these formulae applied equally as well to the high frequency portion of the Q-branch for hydrogen.

In contrast with the case of hydrogen, the Q-branch

of chlorine does not consist of predominantly one line, but consists of many closely overlapping lines. If we assume that each of these lines is of the shape given in Figure (13), each has the same δ and their central frequencies are coincident, then the resultant Q-branch shape will be the same as that of the component lines. Furthermore, its peak intensity will be the sum of the component line peak intensities. In fact, the component lines do not all have the same central frequencies but since they are spread over a very small interval (4 cm^{-1}) the above approximation should be satisfactory.

A plot was consequently made of $1/I(\nu)$ versus $(\Delta\nu)^2$ for the high frequency side of the Cl_2^{35} curve between 551 cm^{-1} and 560 cm^{-1}. This plot is shown in Figure (14) and, since it is a straight line in accordance with equation (3.2) it supports the approximation made above.

From the slope and intercept of the straight line in Figure (14) the constants δ and $1/I_o$, respectively, of equations (3.1) and (3.2) were determined and the remainder of the Q-branch was constructed synthetically by extending equations (3.1) and (3.2) to higher and lower frequencies.

The absorption intensity represented by this synthetic contour was then subtracted from the experimental contour and the approximate shape and position of the O-

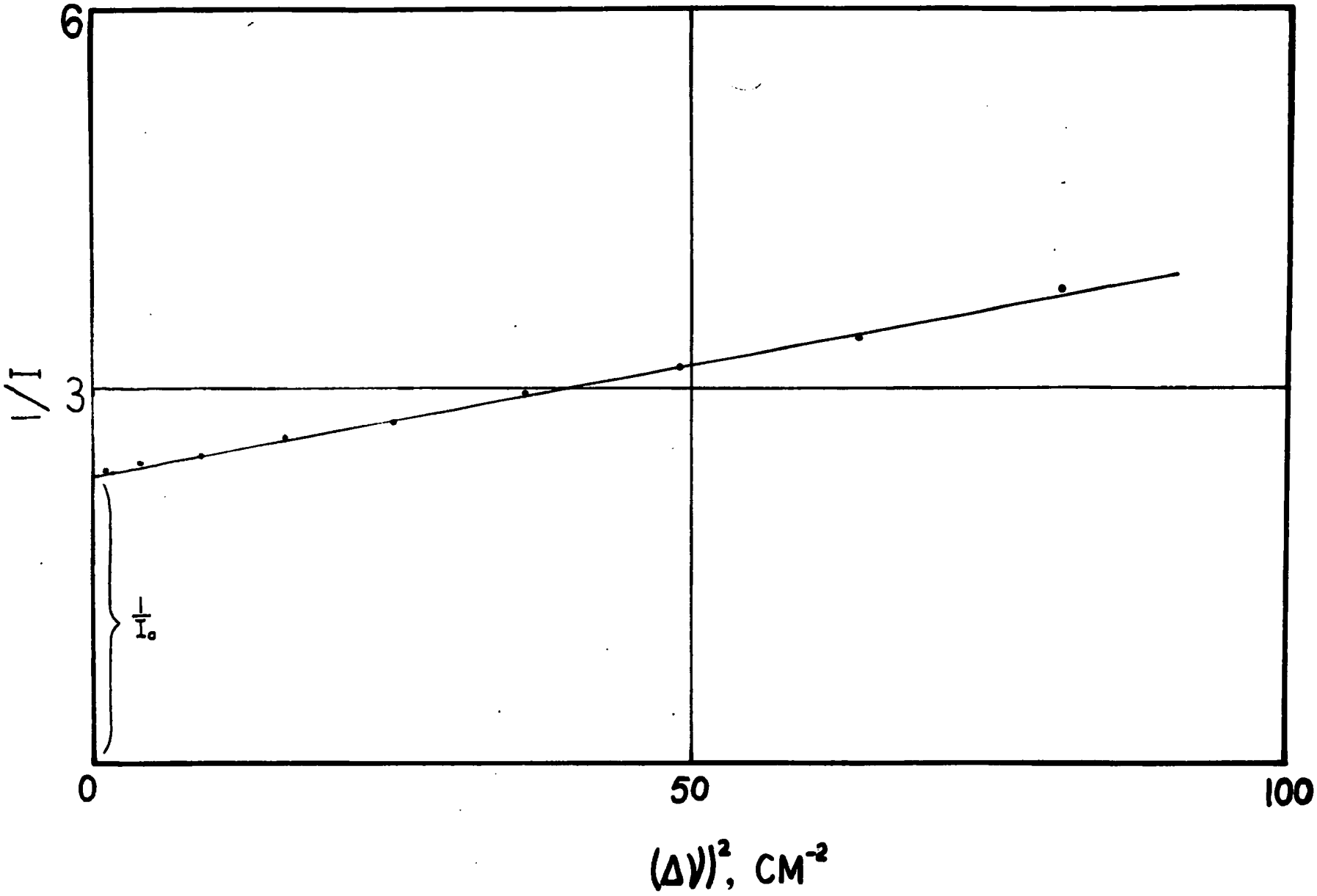

Figure (14): Plot of 1/I(ν) vs $(\Delta\nu)^2$ for Q-branch of pure chlorine contour.

and S-branches determined. The results are shown in Figure (15). The peak of the S-branch occurs at about 585 cm^{-1}. The peak frequency of the O-branch could not be accurately determined but it lies in the interval from 520 cm^{-1} to 527 cm^{-1}. The peaks of these branches are also shifted from their calculated positions. In the case of the S-branch, the shift is about 8 cm^{-1} to higher frequencies. The shift of the O-branch is comparable but to lower frequencies. The ratio of the peak intensities of these two branches is 1 to 1.95 which is considerably different from that expected on the basis of the intensity calculations of Appendix ID. In this respect it is important to stress that the absorption represented by the synthetic Q-branch of Figure (15) is larger than it, in fact, should be, since no attempt could be made to estimate the intensity contribution of the O- and S-branches at the position of the peak of the Q-branch. A compensation for this effect would give rise to increased intensities in the O- and S-branches, but these contributions should be nearly equal so that the anomalous intensity ratio for the latter branches would still exist. Again, this effect may be a reflection of the errors inherent in the method used to extract the absorption due to $Cl^{35}Cl^{37}$ and Cl_2^{37} from the experimental contour. In any case, no conclusions can be drawn till the completion of more accurate work.

From the pure chlorine curves of Figure (9) the

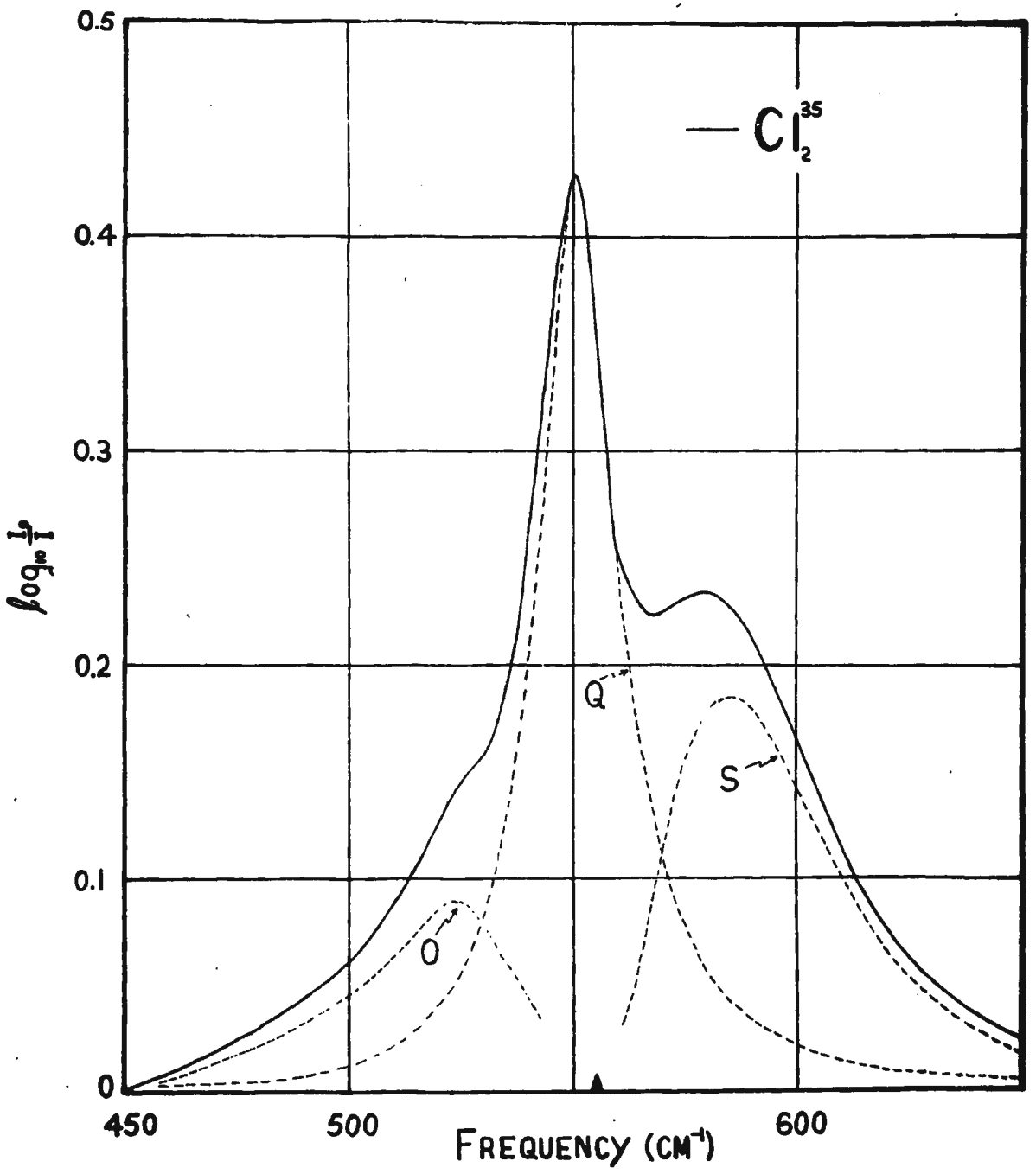

Figure (15): Analysis of Cl_2^{35} contour.

quantity:

$$\alpha_0 = \frac{1}{\ell}\int \ell \log_e I_0/I \, d\nu = \int A' d\nu \qquad (3.3)$$

where ℓ is the path length in cm, was derived by measuring the areas under the curves with a planimeter.

On the basis of the theory of pressure induced absorption developed by Van Kranendonk,[14] an estimation was made of the correction factor for the "apparent induced absorption" and it was found that the contribution was negligible over the range of experimental gas densities.

The experimental values of α_0 were consequently used to obtain the binary and ternary absorption coefficients, α_1 and α_2, which are defined by the relation:

$$\alpha_0 = \int A' d\nu = \alpha_1 \rho_0 \rho_p + \alpha_2 \rho_a \rho_p^2 + \cdots \qquad (3.4)$$

where, again, for the pure gas, $\rho_a \equiv \rho_p$. It is apparent when this equation is rearranged,

$$\frac{\alpha_0}{\rho_a \rho_p} = \frac{1}{\rho_a \rho_p}\int A' d\nu = \alpha_1 + \alpha_2 \rho_p + \cdots$$

that α_1 and α_2 can be determined from the intercept and slope, respectively, of the straight line resulting from the plot of the experimental values of $\frac{\alpha_0}{\rho_a \rho_p}$ versus ρ_p.

This curve, shown in Figure (16), was determined for pure chlorine and the values of the absorption coefficients obtained were:

$$\alpha_1 = 12.2 \times 10^{-3} \text{ cm}^{-1}/\text{cm/Agt}^2$$
$$\alpha_2 = 715 \times 10^{-6} \text{ cm}^{-1}/\text{cm/Agt}^3$$

For purposes of comparison, the corresponding experimental values for hydrogen, obtained at the University of Toronto,[21] are given below:

$$\alpha_1 = 2.42 \times 10^{-3} \text{ cm}^{-1}/\text{cm/Agt}^2$$
$$\alpha_2 = 1.1 \times 10^{-6} \text{ cm}^{-1}/\text{cm/Agt}^3$$

The theory developed by Van Kranendonk[14,15] for the induced absorption of symmetric diatomic molecules shows that the long range part of the intermolecular forces gives rise to an absorption intensity in the pure gas which is proportional to $(Q'\bar{\alpha})^2(Q\bar{\alpha}')^2$, where Q is the molecular quadrupole moment and $\bar{\alpha}$ the molecular polarizability. The primes denote the first rate of change with respect to the internuclear distance. Of these quantities only $\bar{\alpha}$ is known for chlorine (App. II) and it is 5 times larger than that for hydrogen. It is unlikely that any of the other three quantities, Q, Q', $\bar{\alpha}'$, for chlorine is significantly smaller than their counterparts for hydrogen and so it is not surprising that α_1 for chlorine is larger than that for hydrogen.

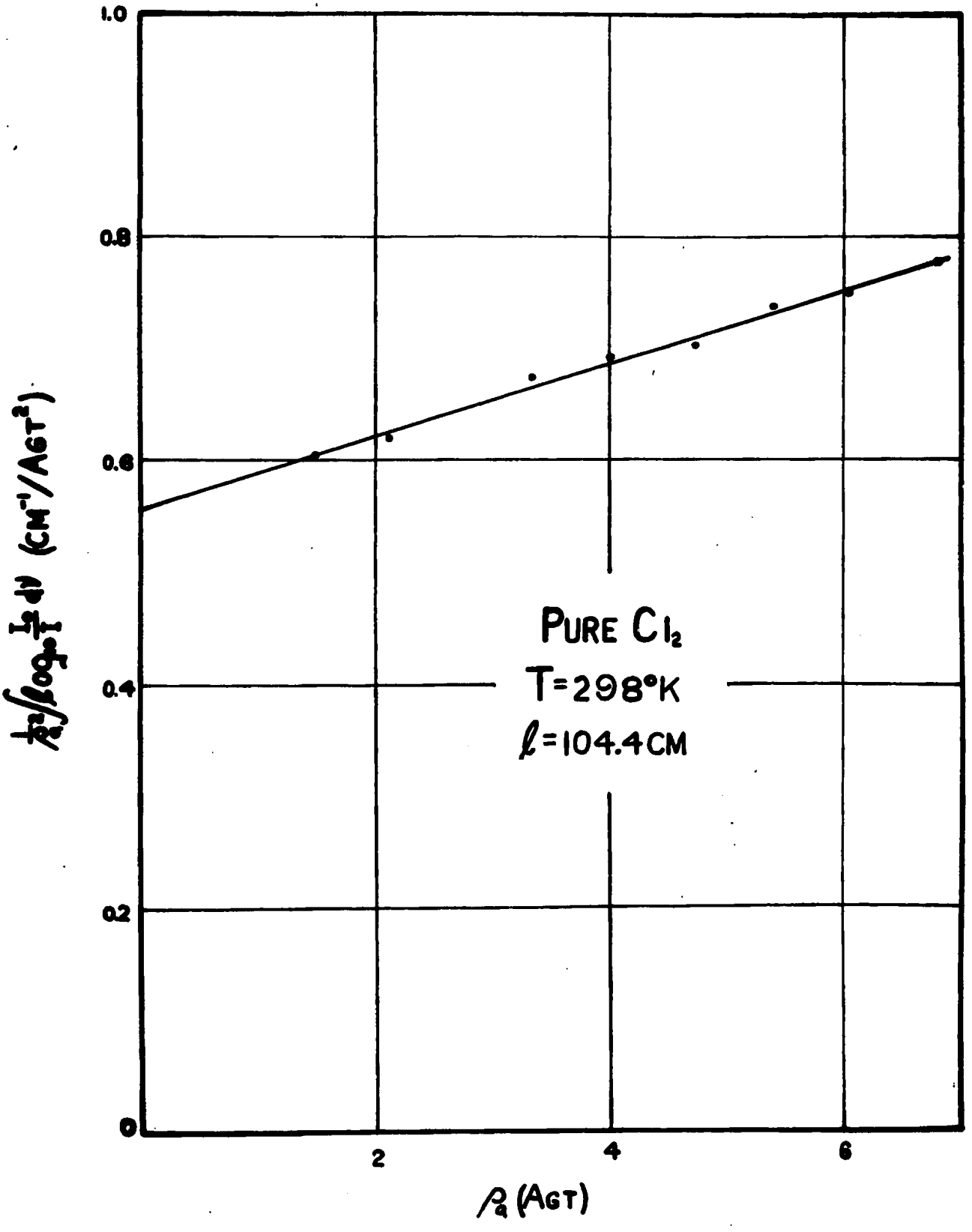

Figure (16): The variation of $1/\rho_a^2 \int \log_{10} I_0/I \, d\nu$ with ρ_a for pure chlorine at 298°K.

The value of α_2 for chlorine, given above, is very large compared with that for hydrogen even allowing for the larger molecular polarizability of chlorine. The value of α_2/α_1 for chlorine is 58.7×10^{-3} Agt^{-1} whereas for hydrogen it is 0.45×10^{-3} Agt^{-1}. In the theory of induced infra-red absorption,[16] Van Kranendonk describes the ternary absorption coefficient α_2, as the sum of three terms:

$$\alpha_2 = \alpha_2^{(1)} + \alpha_2^{(2)} + \alpha_2^{(3)} \qquad (3.5)$$

$\alpha_2^{(3)}$ is due to the non-additive part of the induced dipole moment in clusters of three molecules and is here negligible. $\alpha_2^{(1)}$ arises from clusters of three molecules where each molecule is within the range of the others' intermolecular forces. It is called the "intermolecular force effect", and among other things, it depends on the quantities $\overline{\alpha}$, $\overline{\alpha}'$, Q and Q' in the same manner as does α_1. Therefore, an α_2 for chlorine larger than that for hydrogen is not unexpected. That it should be so very much larger, however, would seem to require an unusual combination of increases in the foregoing quantities.

$\alpha_2^{(2)}$ arises when there are three molecules within the range of each others induced dipole moments. If the configuration of the three molecules is such that molecules 2 and 3 (the perturbing molecules) are never

close together, then the $\alpha_2^{(2)}$ term is negative. For this reason it is called the "cancellation effect". It has been shown by Van Kranendonk[14] that the cancellation effect applies only to "single transitions" and not to "double transitions". In a single transition, one molecule performs both the vibrational and rotational transitions; in a double transition, one molecule of the interacting pair performs the vibrational transition and the other performs the rotational transition. This circumstance offers another possibility for further explaining the very large ratio of α_2/α, for chlorine compared with that for hydrogen. If, for chlorine, conditions are such that $(\bar{\alpha}'Q)$ is much larger than $(\bar{\alpha}\,Q')$ then the intensity of the S- and O-branches of the band would be largely due to double transitions to which the cancellation effect does not apply.

In the case of pure hydrogen at 300°K, the single and double transitions are of very nearly equal intensity and, also, $\alpha_2^{(1)}$ and $\alpha_2^{(2)}$, according to theory, are very nearly equal and opposite in sign, their sum being small and positive. If, as mentioned previously, $(\bar{\alpha}'Q)$ is much larger than $(\bar{\alpha}\,Q')$, for chlorine (even though $\bar{\alpha}_{Cl_2}$ is much greater than $\bar{\alpha}_{H_2}$) then the larger α_1 and the very large α_2 would be understandable. Whether or not the O- and S-branches are predominantly double transitions might be established by observing the spectrum of the liquid or even solid chlorine at high resolution.

As a matter of interest, a value of the molecular diameter of chlorine was calculated using the following approximate relation derived from statistical mechanical considerations of the finite molecular volume (assuming hard sphere molecules):[26]

$$\frac{\alpha_2}{\alpha_1} = \frac{8}{9}\pi D^3 N_o \qquad (3.6)$$

D is the molecular diameter of the perturbing molecule, which in this case is chlorine, and N_o is Loschmidt's number. The resulting value for D was 9Å.

It should be noted that in previous calculations, the molecular diameters of hydrogen, helium, nitrogen and argon were always found to be of the same order of magnitude but slightly smaller than the values obtained from kinetic theory calculations. In this case, however, since the value of the Lennard-Jones σ for chlorine is given as 4.30Å,[22] the calculated value quoted previously is of the same order of magnitude but larger. No explanation is offered for this anomaly.

With reference to the gas mixture contours of Figures (10) and (11), it was found that no quantitative analyses could be attempted because of the great inaccuracies of the contours. These inaccuracies were

considered to be largely, if not wholly, due to decreases in the chlorine density as a result of reaction at high pressure with residual organic impurities in the cell and possibly with the cell itself. It is therefore apparent that, before each gas mixture experiment, the cell should have been purged with a high pressure mixture of chlorine and some foreign gas rather than with 80 p-s-i of pure chlorine as was actually the case.

A Cl_2-He mixture experiment was also carried out but no measurable absorption was observed up to the maximum densities; ρ_a = 4.94 Amagat units, ρ_b = 195 Amagat units.

SUMMARY

The pressure induced fundamental rotation-vibration band of chlorine was observed in the pure gas at 300°K with densities from 1.49 to 6.80 Amagat units, and in Cl_2- A, Cl_2- N_2 gas mixtures up to the maximum densities, ρ_a = 4.05 Amagat units, ρ_ρ = 193 Amagat units. The latter results, however, were inconclusive because of errors due to chemical reaction.

The peak of absorption in the pure gas was found to occur at 549 ± 1 cm^{-1} which is about 6 cm^{-1} lower in frequency than the calculated position for Cl_2^{35}. An approximate contour analysis was performed to determine if this shift was due to absorption resulting from the isotopic molecules $Cl^{35}Cl^{37}$, Cl_2^{37}. The correction resulting from this analysis was about 1 cm^{-1}, so that the peak of absorption due to Cl_2^{35} still showed a red shift of about 5 cm^{-1}.

The binary and ternary absorption coefficients, α_1 and α_2 were found to be 12.2 x 10^{-3} $cm^{-1}/cm/Agt^2$ and 715 x 10^{-6} $cm^{-1}/cm/Agt^3$, respectively. The values of these coefficients are large compared with those of hydrogen, and the value of α_2 particularly so. A possible explanation for the large value of α_2 is proposed, supposing that the rotational branches of the band are largely due to double transitions in which case the cancellation effect does not apply.

APPENDIX I

A. Energy levels and populations of the vibrational levels of Cl_2^{35}.

The molecular constants for Cl_2^{35} as obtained from the literature[23,24] are:

$$\omega_e = 564.9 \text{ cm}^{-1}$$
$$\omega_e x_e = 4.0 \text{ cm}^{-1}$$
$$B_e = 0.2438 \text{ cm}^{-1}$$
$$\alpha_e = 0.0017 \text{ cm}^{-1}$$

ω_e is the "vibrational constant", $\omega_e x_e$ is the "vibrational anharmonicity", B_e is the "rotational constant" and α_e is the "rotation-vibration interaction constant".

The vibrational energy levels, G(v), are given by the formula:

$$G(v) = \omega_e(v + \tfrac{1}{2}) - \omega_e x_e(v + \tfrac{1}{2})^2 + \cdots\cdots$$

where v is the vibrational quantum number. The following values were calculated:

$$G(0) = 281.45 \text{ cm}^{-1}$$
$$G(1) = 838.35 \text{ cm}^{-1}$$
$$G(2) = 1387.25 \text{ cm}^{-1}$$
$$G(3) = 1928.15 \text{ cm}^{-1}$$
$$G(4) = 2461.05 \text{ cm}^{-1}$$

The vibrational, 0 - 1, transition can therefore be

expected to occur at the frequency given by:

$$Q_1(0) = G(1) - G(0) = 556.9 \text{ cm}^{-1}$$

The fractional populations, N_v/N, of the vibrational energy levels are given by:

$$\frac{N_v}{N} = \frac{1}{Q_v} \exp\left\{-\frac{G(v)hc}{kT}\right\}$$

where Q_v is the vibrational partition function:

$$Q_v = \sum_v \exp\left\{-\frac{G(v)hc}{kT}\right\}$$

In this case, it was only necessary to carry the summation to v = 3 since the populations of higher vibrational levels were found to be negligible. The percent populations, as calculated from the values of N_v/N for T = 300°K are given in Table I.

Table I

v	% populations
0	93.00%
1	6.51%
2	0.0046%
3	0.00035%

B. Vibrational isotope shift for $Cl^{35}Cl^{37}$ and Cl_2^{37}.

The constants for isotopic molecules, designated by the right superscript, i, are given by the theory of the "Isotope Effect" as:

$$\omega_e^i = \rho \omega_e$$
$$\omega_e^i x_e^i = \rho^2 \omega_e x_e$$

where ρ is given by:

$$\rho = (\mu/\mu^i)^{\frac{1}{2}}$$

μ being the reduced mass of the lighter molecule (Cl_2^{35}) and μ^i the reduced mass of the heavier molecule($Cl^{35}Cl^{37}$, Cl_2^{37}). For $Cl^{35}Cl^{37}$ we thus have:

$$\omega_e^i = 0.986\omega_e$$
$$= 557.0 \text{ cm}^{-1}$$

$$\omega_e^i x_e^i = 0.972\omega_e x_e$$
$$= 3.9 \text{ cm}^{-1}$$

And for Cl_2^{37}:

$$\omega_e^i = 0.973\omega_e$$
$$= 549.6 \text{ cm}^{-1}$$

$$\omega_e^i x_e^i = 0.947\omega_e x_e$$
$$= 3.8 \text{ cm}^{-1}$$

Using the formula:

$$G^i(v) = \omega_e^i(v + \tfrac{1}{2}) - \omega_e^i x_e^i(v + \tfrac{1}{2})^2 + \text{-----}$$

the zeroth and first vibrational levels are then given by:

$\underline{Cl^{35}Cl^{37}}$: $G(0) = 277.5\ cm^{-1}$

$G(1) = 826.7\ cm^{-1}$

$\underline{Cl_2^{37}}$: $G(0) = 273.9\ cm^{-1}$

$G(1) = 815.8\ cm^{-1}$

The frequencies of the 0 - 1 vibrational transitions are:

$\underline{Cl^{35}Cl^{37}}$: $Q_1(0) = 549.2\ cm^{-1}$

$\underline{Cl_2^{37}}$: $Q_1(0) = 541.9\ cm^{-1}$

These transitions are 7.7 cm^{-1} and 15.0 cm^{-1}, respectively, lower in frequency than the value of $Q_1(0)$ for Cl_2^{35} given in part A.

C. Energy levels and populations of the rotational levels of Cl_2^{35}.

The ground state of the Cl_2^{35} molecule is designated by $^1\Sigma_g^+$, therefore even numbered rotational states are symmetric. The nuclear spin, I, is 3/2 so that the total nuclear spin, T, of the molecule may have the values:

$$T = 2I,\ 2I - 1,\ \text{-----}\ 0$$
$$= 3,\ 2,\ 1,\ 0$$

The values of the nuclear statistical weights are then:

$$g_n = 2T + 1$$
$$= 7,\ 5,\ 3,\ 1$$

Thus, for even numbered states, $g_n^e = 6$, and for odd numbered states, $g_n^o = 10$. The rotational levels for J = 0 to 4

are given below with the appropriate total statistical weights, $g_n x\ g_J = g_n(2J + 1)$:

J			$g_n x\ g_J$	
4	s	———————	6x9=54	para
3	a	———————	10x7=70	ortho
2	s	———————	6x5=30	para
1	a	———————	10x3=30	ortho
0	s	———————	6x1=6	para

The energies, in cm^{-1}, of these levels are given by:

$$F_v(J) = B_vJ(J + 1) - D_vJ^2(J + 1)^2 + \text{----}$$

where v and J are the vibrational and rotational quantum numbers, respectively. The value of B_v is given by:

$$B_v = B_e - \alpha_e(v + \tfrac{1}{2})$$
$$= 0.2438 - 0.0017(v + \tfrac{1}{2})$$

the values for B_e and α_e having been stated previously. The value of D_v is given by:

$$D_v = D_e + \beta_e(v + \tfrac{1}{2})$$

Since no information was available on the values of D_e and β_e, D_v was derived approximately, assuming $\beta_e = 0$, from the following relation:

$$D_v = \frac{4B_v^3}{\omega_e^2}$$

Using this information, the fractional populations, N_J/N, for T = 300°K, were calculated from the following two relations for para and ortho states:

para:
$$N_J/N = \frac{3}{8} \frac{(2J+1)\exp\left\{-\frac{F_o(J)}{kT}\right\}}{\sum_{J\,even} (2J+1)\exp\left\{-\frac{F_o(J)}{kT}\right\}}$$

ortho:
$$N_J/N = \frac{5}{8} \frac{(2J+1)\exp\left\{-\frac{F_o(J)}{kT}\right\}}{\sum_{J\,odd} (2J+1)\exp\left\{-\frac{F_o(J)}{kT}\right\}}$$

These values are given in Table II:

Table II

J	$F_o(J)$	$F_1(J)$	$N_J/N \times 10^3$
0	0	0	0.870
1	0.486	0.480	4.336
2	1.457	1.439	4.315
3	2.915	2.878	9.999
4	4.858	4.796	7.649
5	7.286	7.194	15.388
6	10.201	10.072	10.770
7	13.600	13.429	20.358
8	17.485	17.265	13.599
9	21.855	21.581	24.784

J	$F_o(J)$	$F_1(J)$	$N_J/N \times 10^3$
10	26.708	26.377	16.072
11	32.050	31.652	28.573
12	37.875	37.407	18.135
13	44.184	43.641	31.645
14	50.977	50.355	19.757
15	58.254	57.548	33.953
16	66.015	65.220	20.920
17	74.260	73.371	35.510
18	82.987	82.002	21.641
19	92.198	91.113	36.309
20	101.980	100.702	21.883
21	112.065	110.771	36.395
22	122.722	121.319	21.735
23	133.860	132.346	35.832
24	145.480	143.852	21.221
25	157.579	155.837	34.700
26	170.195	168.301	20.389
27	183.219	181.244	33.096
28	196.578	194.666	19.305
29	210.775	208.567	31.110
30	225.271	222.946	18.022
31	240.245	237.804	28.838
32	255.695	253.141	16.595
33	271.623	268.957	26.389
34	288.026	285.251	15.085
35	304.905	302.023	23.830
36	322.259	319.274	13.546

J	$F_o(J)$	$F_1(J)$	$N_J/N \times 10^3$
37	340.087	337.004	21.272
38	358.388	355.211	12.011
39	377.163	373.897	18.756
40	396.410	393.061	10.535
41	416.128	412.701	16.352
42	436.317	432.823	9.133
43	456.976	453.421	14.090
44	478.105	474.496	7.456
45	499.702	496.050	12.022
46	521.767	518.081	6.626
47	544.299	540.589	10.115
48	567.297	563.575	5.561
49	590.761	587.039	8.433
50	614.689	610.980	4.613
51	639.081	635.398	6.968
52	663.936	660.293	3.782
53	689.252	685.665	5.688
54	715.029	711.514	3.072
55	741.267	737.839	4.599
56	767.963	764.642	2.477
57	795.117	791.921	3.682
58	822.729	819.676	1.965
59	850.797	847.908	2.913
60	879.320	876.616	1.558
61	908.296	905.801	2.352
62	937.726	935.461	1.218
63	967.608	965.597	1.785

J	$F_0(J)$	$F_1(J)$	$N_J/N \times 10^3$
64	997.940	996.210	0.943
65	1028.722	1027.297	1.366
66	1059.953	1058.860	0.717
67	1091.631	1090.899	1.037
68	1123.755	1123.413	0.524
69	1156.324	1156.403	0.785
70	1189.337	1189.867	0.405
71	1222.793	1223.806	0.580
72	1256.690	1258.220	0.303
73	1290.397	1293.041	0.447
74	1325.803	1328.472	0.220
75	1361.017	1364.310	0.328
76	1396.667	1400.621	0.160
77	1432.752	1437.407	0.225
78	1469.271	1474.667	0.123
79	1506.222	1512.401	0.161
80	1543.604	1550.608	0.084

D. Frequencies and relative intensities of the $Q_{1,2}$, S_1 and O_1 lines.

The frequencies, ν , in cm^{-1}, for the appropriate transitions, $\Delta J = +2$, $\Delta J = -2$, $\Delta J = 0$ were calculated from the values of $F_0(J)$ and $F_1(J)$ given in Table II. The relative absorption intensities, I, were then calculated

for the appropriate transitions by means of the relation:

$$I_J \propto S_J \left[\frac{N_J}{N}\right] \nu$$

where the values of the "line strength constant", S_J, are as follows:

$$\Delta J = +2: \quad S_J = \frac{3}{2} \frac{(J + 1)(J + 2)}{(2J + 3)(2J + 1)}$$

$$\Delta J = -2: \quad S_J = \frac{3}{2} \frac{J(J - 1)}{(2J - 1)(2J + 1)}$$

$$\Delta J = 0: \quad S_J = \frac{J(J + 1)}{(2J - 1)(2J + 3)(2J + 1)}$$

These values are given in Tables III, IV, and V for the O-branch ($\Delta J = -2$), the Q-branch ($\Delta J = 0$), and the S-branch ($\Delta J = +2$), respectively.

Table III

$O_1(J)$	ν	I	$O_1(J)$	ν	I
$O_1(0)$	-	0	$O_1(9)$	548.47	4.545
$O_1(1)$	-	0	$O_1(10)$	547.46	2.977
$O_1(2)$	555.44	0.479	$O_1(11)$	546.43	5.334
$O_1(3)$	554.46	1.426	$O_1(12)$	545.40	3.406
$O_1(4)$	553.48	1.210	$O_1(13)$	544.37	5.972
$O_1(5)$	552.49	2.576	$O_1(14)$	543.33	3.743
$O_1(6)$	551.50	1.869	$O_1(15)$	542.29	6.452
$O_1(7)$	550.49	3.621	$O_1(16)$	541.23	3.985
$O_1(8)$	549.49	2.462	$O_1(17)$	540.19	6.776

$O_1(J)$	ν	I	$O_1(J)$	ν	I
$O_1(18)$	539.13	4.135	$O_1(44)$	511.62	1.398
$O_1(19)$	538.07	6.946	$O_1(45)$	510.62	2.251
$O_1(20)$	536.92	4.188	$O_1(46)$	509.63	1.239
$O_1(21)$	535.95	6.970	$O_1(47)$	508.65	1.888
$O_1(22)$	534.88	4.164	$O_1(48)$	507.68	1.037
$O_1(23)$	533.81	6.864	$O_1(49)$	506.73	1.570
$O_1(24)$	532.74	4.065	$O_1(50)$	505.79	0.856
$O_1(25)$	531.67	6.644	$O_1(51)$	504.86	1.293
$O_1(26)$	530.59	3.902	$O_1(52)$	503.94	0.701
$O_1(27)$	529.52	6.331	$O_1(53)$	503.05	1.053
$O_1(28)$	528.44	3.690	$O_1(54)$	502.16	0.568
$O_1(29)$	527.37	5.942	$O_1(55)$	501.30	0.849
$O_1(30)$	526.29	3.439	$O_1(56)$	500.45	0.457
$O_1(31)$	525.22	5.498	$O_1(57)$	499.62	0.678
$O_1(32)$	524.19	3.161	$O_1(58)$	498.71	0.349
$O_1(33)$	523.08	5.021	$O_1(59)$	498.02	0.535
$O_1(34)$	522.02	2.867	$O_1(60)$	497.26	0.286
$O_1(35)$	520.95	4.523	$O_1(61)$	496.51	0.431
$O_1(36)$	519.89	2.425	$O_1(62)$	495.79	0.223
$O_1(37)$	518.84	4.028	$O_1(63)$	495.09	0.326
$O_1(38)$	517.79	2.271	$O_1(64)$	494.42	0.172
$O_1(39)$	516.74	3.542	$O_1(65)$	493.78	0.249
$O_1(40)$	515.70	1.987	$O_1(66)$	493.16	0.131
$O_1(41)$	514.67	3.079	$O_1(67)$	492.57	0.189
$O_1(42)$	513.64	1.663	$O_1(68)$	492.01	0.095
$O_1(43)$	512.63	2.646			

Table IV

$Q_1(J)$	ν	I	$Q_1(J)$	ν	I
$Q_1(0)$	556.90	0	$Q_1(26)$	555.04	2.832
$Q_1(1)$	556.89	0.966	$Q_1(27)$	554.93	4.596
$Q_1(2)$	556.88	0.687	$Q_1(28)$	554.81	2.680
$Q_1(3)$	556.86	1.485	$Q_1(29)$	554.69	4.318
$Q_1(4)$	556.84	1.106	$Q_1(30)$	554.56	2.501
$Q_1(5)$	556.81	2.197	$Q_1(31)$	554.46	4.000
$Q_1(6)$	556.77	1.526	$Q_1(32)$	554.35	2.301
$Q_1(7)$	556.73	2.872	$Q_1(33)$	554.23	3.658
$Q_1(8)$	556.68	1.687	$Q_1(34)$	554.12	2.091
$Q_1(9)$	556.63	3.112	$Q_1(35)$	554.02	3.303
$Q_1(10)$	556.57	2.241	$Q_1(36)$	553.92	1.877
$Q_1(11)$	556.50	3.650	$Q_1(37)$	553.82	2.947
$Q_1(12)$	556.43	2.332	$Q_1(38)$	553.72	1.663
$Q_1(13)$	556.36	4.092	$Q_1(39)$	553.63	2.597
$Q_1(14)$	556.28	2.568	$Q_1(40)$	553.55	1.459
$Q_1(15)$	556.19	4.430	$Q_1(41)$	553.48	2.264
$Q_1(16)$	556.10	2.739	$Q_1(42)$	553.41	1.264
$Q_1(17)$	556.01	4.665	$Q_1(43)$	553.34	1.950
$Q_1(18)$	555.92	2.851	$Q_1(44)$	553.29	1.032
$Q_1(19)$	555.82	4.796	$Q_1(45)$	553.25	1.633
$Q_1(20)$	555.71	2.897	$Q_1(46)$	553.21	0.917
$Q_1(21)$	555.61	4.828	$Q_1(47)$	553.19	1.396
$Q_1(22)$	555.50	2.889	$Q_1(48)$	553.18	0.769
$Q_1(23)$	555.39	4.981	$Q_1(49)$	553.18	1.167
$Q_1(24)$	555.27	2.949	$Q_1(50)$	553.19	0.644
$Q_1(25)$	555.16	4.821	$Q_1(51)$	553.22	0.964

$Q_1(J)$	ν	I	$Q_1(J)$	ν	I
$Q_1(52)$	553.26	0.523	$Q_1(61)$	554.40	0.326
$Q_1(53)$	553.31	0.787	$Q_1(62)$	554.64	0.169
$Q_1(54)$	553.38	0.425	$Q_1(63)$	554.89	0.247
$Q_1(55)$	553.47	0.636	$Q_1(64)$	555.17	0.130
$Q_1(56)$	553.58	0.343	$Q_1(65)$	555.46	0.189
$Q_1(57)$	553.70	0.509	$Q_1(66)$	555.81	0.100
$Q_1(58)$	553.85	0.272	$Q_1(67)$	556.17	0.144
$Q_1(59)$	554.01	0.404	$Q_1(68)$	556.58	0.073
$Q_1(60)$	554.20	0.216			

Table V

$S_1(J)$	ν	I	$S_1(J)$	ν	I
$S_1(0)$	558.34	0.486	$S_1(12)$	569.38	4.176
$S_1(1)$	559.29	1.455	$S_1(13)$	570.26	7.260
$S_1(2)$	560.24	1.243	$S_1(14)$	571.14	4.519
$S_1(3)$	561.18	2.672	$S_1(15)$	572.02	7.746
$S_1(4)$	562.11	1.954	$S_1(16)$	572.89	4.763
$S_1(5)$	563.04	3.817	$S_1(17)$	573.75	8.071
$S_1(6)$	563.96	2.616	$S_1(18)$	574.61	4.912
$S_1(7)$	564.88	4.868	$S_1(19)$	575.47	8.232
$S_1(8)$	565.79	3.216	$S_1(20)$	576.33	4.957
$S_1(9)$	566.70	5.808	$S_1(21)$	577.18	8.240
$S_1(10)$	567.60	3.740	$S_1(22)$	578.03	4.919
$S_1(11)$	568.49	6.610	$S_1(23)$	578.88	8.106

$S_1(J)$	ν	I	$S_1(J)$	ν	I
$S_1(24)$	579.72	4.800	$S_1(43)$	595.97	3.221
$S_1(25)$	580.56	7.848	$S_1(44)$	596.88	1.706
$S_1(26)$	581.41	4.612	$S_1(45)$	597.79	2.754
$S_1(27)$	582.25	7.487	$S_1(46)$	598.71	1.520
$S_1(28)$	583.09	4.368	$S_1(47)$	599.64	2.322
$S_1(29)$	583.93	7.041	$S_1(48)$	600.58	1.278
$S_1(30)$	584.77	4.076	$S_1(49)$	601.54	1.940
$S_1(31)$	585.61	6.532	$S_1(50)$	602.50	1.063
$S_1(32)$	586.46	3.761	$S_1(51)$	603.48	1.607
$S_1(33)$	587.30	5.984	$S_1(52)$	604.48	0.874
$S_1(34)$	588.15	3.423	$S_1(53)$	605.49	1.316
$S_1(35)$	589.00	5.411	$S_1(54)$	606.51	0.712
$S_1(36)$	589.85	3.078	$S_1(55)$	607.55	1.067
$S_1(37)$	590.71	4.837	$S_1(56)$	608.65	0.575
$S_1(38)$	591.57	2.733	$S_1(57)$	609.69	0.856
$S_1(39)$	592.44	4.272	$S_1(58)$	610.79	0.458
$S_1(40)$	593.31	2.401	$S_1(59)$	611.90	0.680
$S_1(41)$	594.19	3.730	$S_1(60)$	613.04	0.364
$S_1(42)$	595.08	2.086			

E. <u>Isotope shift of maximum intensity lines.</u>

As stated in part C, the rotational levels, $F_v(J)$, are given by:

$$F_v(J) = B_vJ(J + 1) - D_vJ^2(J + 1)^2 + \text{-----}$$

where:

$$B_v = B_e - \alpha_e(v + \tfrac{1}{2})$$

$$D_v = D_e + \beta_e(v + \tfrac{1}{2})$$

The values of the constants B_e, α_e, D_e, and β_e for isotopic molecules are given by:

$$B_e^i = \rho^2 B_e \qquad D_e^i = \rho^4 D_e$$

$$\alpha_e^i = \rho^3 \alpha_e \qquad \beta_e^i = \rho^5 \beta_e$$

Since the $F_v(J)$ terms are small compared with the $G(v)$ terms, however, the rotational isotope shift is much less than the vibrational isotope shift and was neglected in the present work.

The frequencies of the maximum intensity lines, $O_1(21)$, $Q_1(23)$ and $S_1(21)$ for $Cl^{35}Cl^{37}$ and Cl_2^{37} were calculated only on the basis of the vibrational isotope shifts given in part B. The frequencies for all three isotopic molecules are given in Table VI.

Table VI

	$O_1(21)$	$Q_1(23)$	$S_1(21)$
Cl_2^{35}	535.95	555.39	577.18
$Cl^{35}Cl^{37}$	528.25	547.69	569.48
Cl_2^{37}	520.95	540.39	562.18

APPENDIX II

Polarizability of chlorine.

The following experimental values of λ^{-2} (in Å^{-2}) versus (n - 1), n being the refractive index, were obtained from the literature:[25]

λ^{-2}	(n - 1)
0.0434×10^{-6}	791.66×10^{-6}
0.03875×10^{-6}	787.91×10^{-6}
0.03685×10^{-6}	786.51×10^{-6}
0.03465×10^{-6}	784.00×10^{-6}
0.03005×10^{-6}	781.35×10^{-6}
0.02980×10^{-6}	781.21×10^{-6}
0.02415×10^{-6}	777.03×10^{-6}
0.02225×10^{-6}	775.63×10^{-6}

Together with the above values, the following empirical relation was also stated to represent the variation of λ^{-2} with (n - 1) for chlorine:

$$(n - 1)10^6 = \frac{\beta'}{\mu' - \lambda_\mu^{-2}} + \frac{\beta''}{\mu'' - \lambda_\mu^{-2}}$$

For the purposes of the present calculations, $\beta'' = \mu'' = 0$, $\beta' = 81{,}257$, $\mu' = 106.99$. λ_μ is the wavelength in microns. The curve resulting from this relation, however, was not considered to be a good fit for the experimental points.

Figure (i) shows the plot of the experimental values listed above and the curve that was considered to be the best fit.

Assuming $\lambda^{-2} = 0$ for $\lambda = 18\mu = 180{,}000\text{Å}$, the curve of Figure (i) gives the value of $(n - 1)$ as 759.5×10^{-6}. Using this value of $(n - 1)$, $\bar{\alpha}$ was calculated from the Clausius-Mosotti relation:

$$\frac{(n + 1)(n - 1)}{(n^2 + 2)} = \frac{4}{3}\pi \bar{\alpha}\rho$$

where ρ is the gas density. This equation was approximated by assuming $(n + 1) = 2$ and $(n^2 + 2) = 3$. The equation thus becomes:

$$(n - 1) = 2\pi \bar{\alpha}\rho$$

for $\rho = 1$, this relation gives:

$$\bar{\alpha} = 0.0001207 \text{ molecule}^{-1}$$

or, dividing by Loschmidt's number:

$$\bar{\alpha} = 4.49 \times 10^{-24} \text{ cm}^3.$$

may also be expressed in terms of the Bohr radius, a_o:

$$\bar{\alpha} = 30.4 a_o^3 .$$

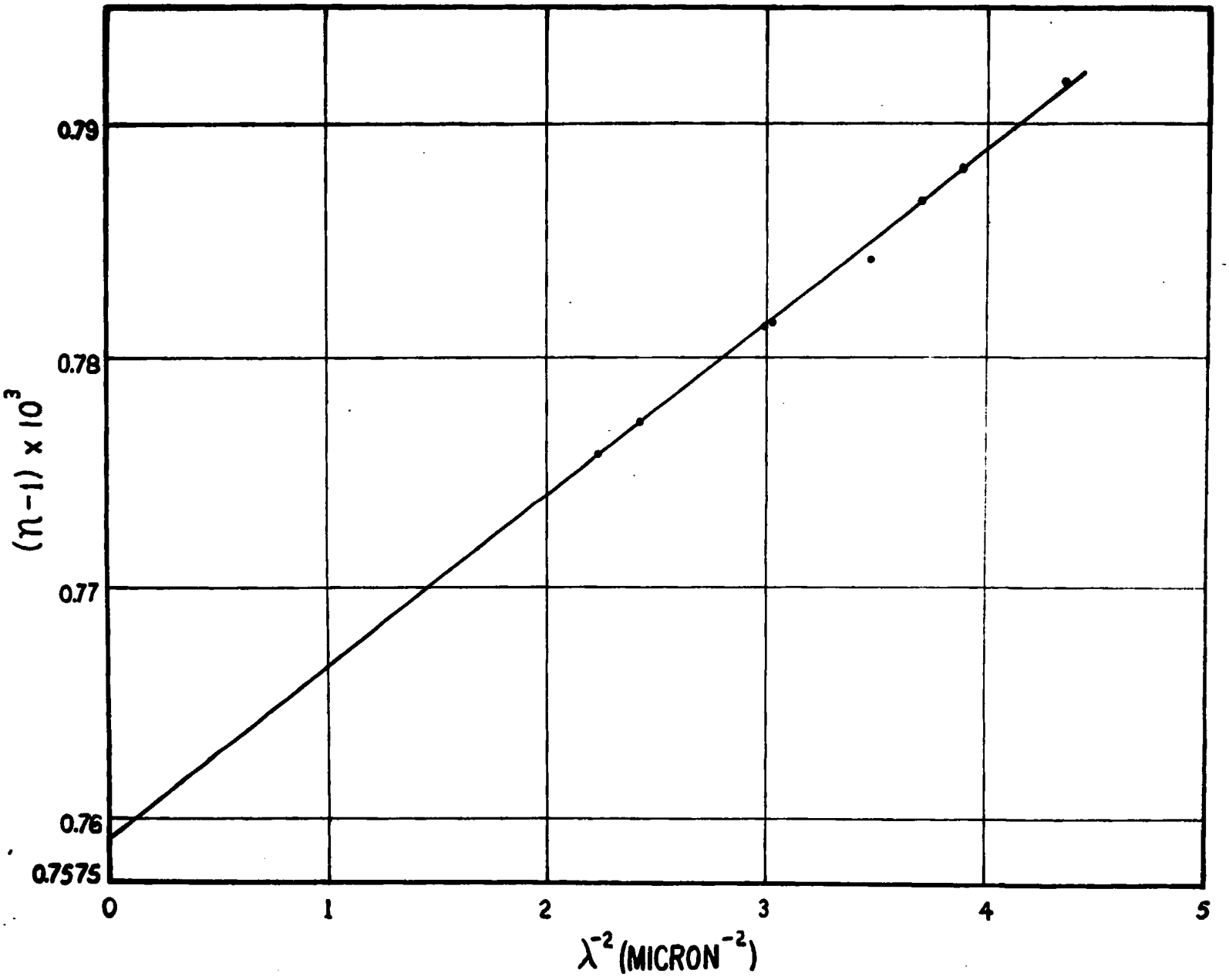

Figure(i): The variation of n-1 with λ^{-2} for pure chlorine.

ACKNOWLEDGEMENTS

The research described in this thesis was supervised by Dr. J. L. Hunt whose active participation in the experimental work and help in the preparation of the thesis are greatly appreciated.

The assistance offered by Mr. C. M. Stevenson in the processing of diagrams for the thesis is gratefully acknowledged.

The skilful work of Mr. W. Gordon and the staff of the machine shop was of great assistance throughout the course of the research.

The author is also indebted to the following people who have offered advice and assistance from time to time during the preparation of the thesis: Dr. C. W. Cho, Mr. C. Snook, Mrs. D. R. Hiscock.

BIBLIOGRAPHY

1. Welsh, H.L.; Crawford, M.F.; Locke, J.L.:
   Phys. Rev. 76 580 (1949).
2. Crawford, M.F.; Welsh, H.L.; Locke, J.L.; MacDonald, J.C.F.:
   Phys. Rev. 80 469 (1950).
3. Hare, W.F.J.; Welsh, H.L.:
   Can. J. Phys. ~~35~~ 36, 88 (1957 8).
4. Kiss, Z.J.; Gush, H.P.; Welsh, H.L.:
   Can. J. Phys. 37 362 (1959).
5. Carswell, A.: Ph.D. Thesis, University of Toronto (1960).
6. Wohl, K.: Z. Phys. Chem. 133 305 (1928).
7. Comings, E.W.:
   "High Pressure Technology", McGraw-Hill (1956)
8. Michels, A.; Wouters, H.; DeBoer, J.:
   Physica 3 585 (1936).
9. Michels, A.; Wijker, H.; Wijker, H.:
   Physica 15 627 (1949).
10. Michels, A.; Wouters, H.:
    Physica 8 923 (1941).
11. Sawyer, R.A.:
    "Experimental Spectroscopy" Edition 2, Prentice-Hall (1956).
12. Dickey, F.P.; Rogge, W.H.:
    Applied Optics 4 538 (1962).
13. Mier, A.O.; Hanson, E.E.:
    Phys. Rev. 50 722 (1936).

14. Van Kranendonk, J.:
Physica 23 825 (1957).
15. Van Kranendonk, J.:
Physica 24 347 (1958).
16. Van Kranendonk, J.:
Physica 25 337 (1959)
17. May, A.D.; Degen, V.; Stryland, J.C.; Welsh, H.L.:
Can. J. Phys. 39 1769 (1961).
18. Buckingham, A.D.:
Proc. Roy. Soc. A248 169 (1958).
19. Buckingham, A.D.:
Trans. Far. Soc. 58 449 (1962).
20. Kiss, Z.J.; Welsh, H.L.:
Can. J. Phys. 37 1249 (1959).
21. Hunt, J.L.:
Ph.D. Thesis, University of Toronto (1959).
22. Hirschfelder, J.O.; Curtiss, C.F.; Bird, R.B.:
"Molecular Theory of Gases and Liquids", Wiley, (1954).
23. Herzberg, G.:
"Spectra of Diatomic Molecules", Edition 2, Van Nostrand (1959)
24. "Landolt - Bornstein", Edition 6, Springer-Verlag, (1955).
25. Cuthbertson, C.; Cuthbertson, M.:
Roy. Soc. London Phil. Trans. 213 1, 14.
26. Chisholm, D.A.; Welsh, H.L.: Can. J. Phys. 32 291 (1954).

15629